Technical Note

1969-27

T. S. Seay
A. H. Huntoon

A LES-5 Beacon Receiver

1 May 1969

Lincoln Laboratory

MASSACHUSETTS INSTITUTE OF TECHNOLOGY

Lexington, Massachusetts

AD692437

MASSACHUSETTS INSTITUTE OF TECHNOLOGY

LINCOLN LABORATORY

A LES-5 BEACON RECEIVER

T. S. SEAY
A. H. HUNTOON

Group 62

TECHNICAL NOTE 1969-27

1 MAY 1969

LEXINGTON   MASSACHUSETTS

ABSTRACT

A functional description of a communications satellite beacon receiver is presented. The system, designed primarily for LES-5/6, is capable of reliable unattended operation, and provides a frequency and time reference for fixed and highly mobile satellite communications terminals.

Theoretical and experimental data are given, with particular emphasis on automatic acquisition and tracking of the satellite beacon signal at low signal-to-noise-density ratios under adverse channel conditions.

iii

CONTENTS

GLOSSARY

AM	Amplitude modulation
BPMF	Bandpass matched filter
°K	Degree(s) Kelvin
EIRP	Effective isotropically radiated power
HLDC	High level downconverter
IL	Insertion loss
LES	Lincoln Experimental Satellite
LPF	Lowpass filter
LPMF	Lowpass matched filter
NF	Noise figure
P_r/N_o	Signal-to-noise-density ratio
RFI	Radio frequency interference
RHCP	Right-hand circularly polarized
TATS	Tactical Transmission System
S/N	Signal-to-noise ratio
VCO	Voltage-controlled oscillator
VCXO	Voltage-controlled crystal oscillator

A LES-5 BEACON RECEIVER

I. INTRODUCTION

Lincoln Experimental Satellites 5 and 6 (LES-5 and -6) radiate a
narrowband UHF beacon signal suitably modulated to provide a frequency and
time reference, together with auxiliary telemetry data, for communications
terminals using the satellites. To use the information transmitted on a bea-
con frequency, a terminal must be equipped with a special beacon receiver.
In many applications the receiver must operate under channel conditions con-
siderably less than ideal.

This Technical Note describes a beacon receiver that provides reliable un-
attended operation for fixed and highly mobile terminals. As such, the receiver
can acquire and track the satellite beacon signal automatically at low signal-to-
noise ratios in the presence of such channel perturbations as multipath, strong
in-band RFI, and doppler frequency shifts. The receiver, expressly designed
to accommodate LES-5 signal levels as seen by a nondirectional antenna, is
quite complex. A design based on the higher beacon effective isotropically
radiated power (EIRP) of LES-6 could be substantially simpler.

The receiver described can reliably acquire a beacon signal within one
minute at a received signal-to-noise-density ratio (P_r/N_o) of 30 db (Hz), and
maintain coherent tracking down to a P_r/N_o below 20 db (Hz). The standard
deviation of the time jitter is less than 25 μsec at the latter P_r/N_o. A sum-
mary of the major technical characteristics is given in Table 1. Clearly,
the receiver has applicability to many other timebase synchronization problems.

Several of these receivers were built and tested during the last two years.
As shown in Fig. 1, panel controls and indicators were included to facilitate
testing.

The body of this Note describes beacon signal characteristics and receiver
functions, together with theoretical and experimental performance. Detailed
technical discussions appear in the appendices.

TABLE 1
UHF BEACON RECEIVER CHARACTERISTICS

1. Acquisition Mode
   a. Frequency search range: ±1 kHz
   b. Frequency search rate: +37 Hz/sec
   c. Probability of missing correct frequency on any one sweep:
      less than 0.1 for P_r/N_o = 30 db (Hz)
   d. Average time from reset to completion of synchronization:
      35 sec for P_r/N_o = 30 db (Hz)
   e. Frequency tracking rate: ±10 Hz/sec for P_r/N_o = 30 db (Hz)
   f. Maximum pause for fade recovery: 8 sec
   g. Automatic switching to monitor mode when acquisition complete

2. Monitor Mode
   a. Average time to loss-of-lock: 7 hr for P_r/N_o = 23 db (Hz),
      230 yr for P_r/N_o = 29 db (Hz)
   b. Peak time jitter in a 2-min interval: less than ±30 μsec for
      P_r/N_o = 20 db (Hz)
   c. Maximum time tracking rate: ±5 μsec/sec
   d. Maximum pause for fade recovery: 8 sec
   e. Delay after loss-of-lock before automatic reversion to
      Acquisition Mode (coherent search duration): 60 sec
   f. Probability of false start of coherent search: $<10^{-10}$ for
      P_r/N_o = 20 db (Hz)

3. General
   a. Noise figure: 3 db
   b. Overload level: −55 dbw within ±13 MHz of beacon frequency
   c. Tunability: programmable over a 1 MHz range on 5-kHz centers
        LES-5 beacon carrier frequency   228.43 MHz
        LES-6 beacon carrier frequency   254.14 MHz
   d. Long term frequency stability: ±1 part in 10^7 per 24 hr
   e. IF selectivity: 60 db rejection at F_c ± 6.5 kHz
   f. Power required: 175 watts, single phase, 115 vac, 50 − 400 Hz
   g. Size: Receiver $25\frac{1}{2} \times 19 \times 7$ in.; Power supply $21\frac{1}{2} \times 19 \times 5\frac{1}{4}$ in.
   h. Weight: Receiver 46 lb; Power supply 66 lb

4. Outputs
   a. Synchronized beacon timing data (serial and parallel)
   b. Synchronized 1 MHz clock
   c. Status indicators (10)
   d. P_r/N_o, Received power level, and frequency meters
   e. Demodulated telemetry
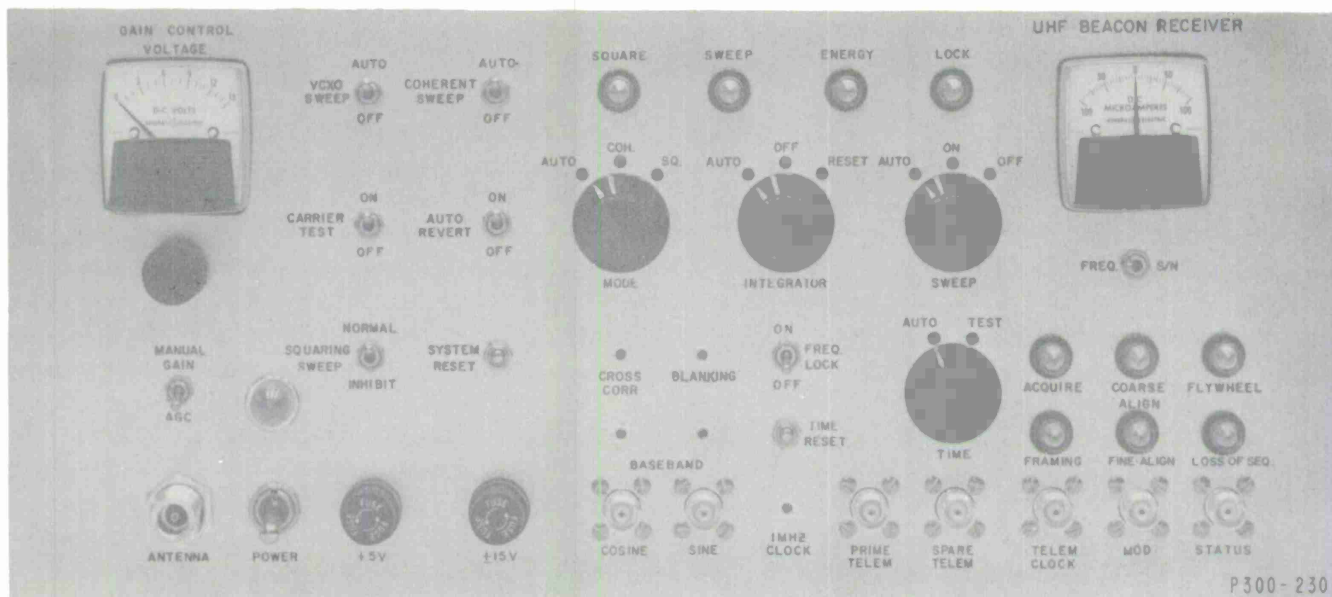   f. Simulated beacon modulation

Fig. 1.   LES-5/6 beacon receiver front panel.

II.   BEACON SIGNAL CHARACTERISTICS

The LES-5 timing beacon is an RF carrier slightly above the edge of the satellite downlink frequency band, biphase modulated with an interlaced set of timing signals.   The EIRP in the beacon signal is approximately 3 watts.[1] The LES-6 beacon is similar, but with an EIRP of approximately 30 watts.[2]

A.   Available Signal-to-Noise-Density Ratio

The nominal downlink power budget for a mobile terminal with a blade antenna using LES-5 signals is shown in Table 2.   The system noise temperature is taken as 700°K, representative of operation over rural land with a 3-db receiver noise figure.[3]   Irregularities in the antenna pattern can result in lower gains.

Three primary sources of downlink degradation are encountered occasionally:

1.   Operation over large cities can result in system noise temperatures of 10,000°K (Ref. 3).   Fortunately, such noise is important only for terminals within about three city radii of the urban border.

3

TABLE 2
UHF BEACON NOMINAL DOWNLINK POWER BUDGET

Satellite RHCP EIRP	+5 dbw
Downlink path loss (quasi-synchronous orbit)	−172 db
Receiver antenna gain*	0 db
Received power, P_r	−167 dbw
Noise power density, N_o	−200 dbw/Hz
P_r/N_o	33 db (Hz)

*Gain is measured relative to an isotropic RHCP antenna. See Ref. 4 for further characterization of simple antennas on large aircraft.

2. Narrowband RFI from such sources as lower band transmitter harmonics can be of sufficient strength to override completely the satellite signal. For reliable operation, the receiver must not lock onto such signals.

3. Multipath fading can occur over water or polar ice. Early experiments indicated this fading could be very severe,[5] but later measurements indicate fading of only 5 db need be considered.[6]

Several features were included to ensure that the receiver behaves gracefully and recovers rapidly in the presence of such unfavorable conditions. However, comparison of the nominal downlink calculation (Table 2) with the receiver characteristics listed in Table 1 indicates little margin is available for initial acquisition of the LES-5 beacon signal.

Since the EIRP of LES-6 is 10 db higher than that of LES-5, operation with LES-6 should be very reliable.

B.   Frequency Uncertainties

Three sources contribute to uncertainty in the effective frequency at which the beacon signal is received:

1.   Error in the satellite beacon oscillator
2.   Doppler frequency shift on the satellite-mobile terminal link (for a quasi-synchronous satellite, this shift is induced primarily by the motion of the terminal)
3.   Error in the terminal's receiver local oscillator.

For the first of these sources, the satellite oscillator on LES-5 was expected to be within ± 2 parts in 10^6 of its nominal frequency (this allows one part in 10^6 for variations with temperature, one part in 10^6 for aging).* Subsonic aircraft contribute a maximum of one part in 10^6 doppler shift. Compared to these, the local oscillators in the terminal should contribute negligible error (less than one part in 10^7). An upper bound, then, for the received frequency uncertainty is ± 4 parts in 10^6, or roughly $\pm 1000\,Hz$ at the expected beacon frequency. This is the range over which the beacon receiver must be able to acquire a received signal.

The maximum expected relative drift in modulation timing is $1\,\mu sec/sec$, corresponding to a doppler shift on one part in 10^6. The relative drift in frequency will almost always be less than $8\,Hz/sec$, corresponding to a maximum acceleration of $1\,g$ in the direction of the satellite. The timing drift requirement is easily met, but the frequency drift requirement limits the minimum P_r/N_o.

C.   Modulation Structure

The function of the modulating signal is to provide a timing reference with resolution better than one millisecond;† and ambiguity, or repeat cycle, greater

---

* Measurements to date indicate this goal was achieved.[1]

† This particular value is for AJ-TATS. The achievable resolution depends on the available P_r/N_o. For the P_r/N_o's of interest, it turned out to be possible to provide two orders of magnitude greater resolution at no additional cost.

than one day. The modulation structure must allow rapid, unambiguous acquisition of the signal by a receiving station having no a priori knowledge of time.

A suitable signal structure is generated by biphase modulating an RF carrier with a set of interlaced binary sequences of properly chosen period.[7] The particular structure chosen for the LES-5 beacon is shown in Fig. 2. The modulation format consists of frames of 10 msec duration, each of which is divided into eight 1.25 msec pulse intervals.
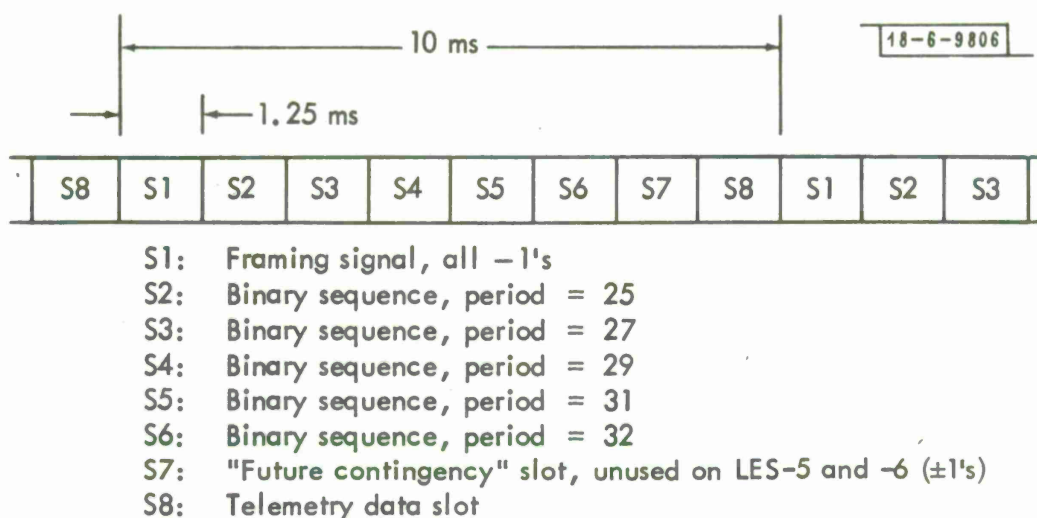

S1: Framing signal, all −1's
S2: Binary sequence, period = 25
S3: Binary sequence, period = 27
S4: Binary sequence, period = 29
S5: Binary sequence, period = 31
S6: Binary sequence, period = 32
S7: "Future contingency" slot, unused on LES-5 and −6 (±1's)
S8: Telemetry data slot

Fig. 2. Beacon modulation structure.

The first slot (pulse interval) of each frame contains a signal that is always −1. This signal has low correlation with the other sequences and is used by the receiver to quickly and unambiguously acquire framing. Slots S2 through S6 contain binary (±1) sequences with periods 25, 27, 29, 31 and 32, respectively. Because these periods are relatively prime, the period of the interlaced sequence is the product of the individual periods, or 19,418,400 frames. Since each frame has a duration of 10 msec, the period in time is thus 194,184 seconds, or approximately $2\frac{1}{4}$ days.

The binary sequences chosen were selected largely on the basis of simplicity of the logic. However, the associated correlation functions are suitable for unambiguous acquisition.

Slot S7 provides "growth potential." In LES-5 this slot is occupied by alternating +1's and −1's.

Slot S8 carries bit-to-bit differential telemetry in the standard LES format. In LES-5 this telemetry transmission is redundant in that the same telemetry data are radiated on a separate frequency to provide a telemetry system as independent as possible of the remainder of the satellite.

The beacon modulation format has the advantage of simplicity in both concept and implementation. Once the receiver establishes framing, it must determine the phase or epoch of five short binary sequences. However, the interlaced structure makes each of these determinations independent, so that they may proceed in parallel, if desired, to increase the speed of acquisition. The shortness of each sequence assures rapid acquisition of the individual sequences.

The time resolution afforded by this modulation structure is related directly to the pulse length (1.25 msec). The ultimate achievable resolution is limited by the signal-to-noise-density ratio at the receiver; however, successful acquisition of the time sequences implies synchronization to a fraction of a pulse period, say to the order of 0.25 msec.

III. FUNCTIONAL DESCRIPTION

The primary function of the beacon receiver is to deliver to a communications terminal the frequency and timing information contained in the received beacon signal. To perform this function, however, the receiver must first find and lock onto the received signal. This is the most difficult part of its task, and accounts for a substantial part of its complexity. The acquire mode, in which the receiver carries out this function, is described in part A of this section.

Once frequency, phase, and time have been acquired by the receiver, it switches to the monitor mode to verify continuously that alignment is maintained. The signal-to-noise-density ratio necessary for operation in the monitor mode is considerably less than that required for initial acquisition. In typical applications the receiver will almost always be in the monitor mode. The monitor mode is described in part B of this section.

Various auxiliary functions were included in the receiver to provide information of interest in ground and flight testing, and to facilitate verification of proper functioning. A demodulator that extracts telemetry information from slot S8 was also included. These provisions are described briefly in part C.

The following discussion outlines the principles of beacon receiver operation. For convenience we explain signal processing in terms of bandpass representations. However, the actual equipment (as described in Appendix A) was realized almost entirely at baseband.

A.   Acquire Mode

Acquisition of the beacon signal occurs in two distinct stages:

1.   The receiver adjusts its primary frequency standard to coincide in RF frequency and phase with the received signal.

2.   Framing time is established and the receiver binary sequence generators (replicas of those in the satellites) are aligned with the modulation on the received signal.

Phase acquisition permits coherent correlation techniques to be used in sequence alignment, which in turn permits reliable acquisition at lower signal-to-noise-density ratios than possible with simpler approaches. At the initial acquisition design point, approximately the same average time is required to complete each stage.

1.   Frequency and Phase Acquisition

Acquisition in frequency and phase is somewhat complicated because the biphase modulated satellite beacon signal has little real carrier component. A "reconstructed" carrier is generated in a conventional manner by passing the received signal through a square law device. This reconstructed carrier is used for frequency and phase synchronization as long as the receiver is in the acquire mode.

8

To see how the carrier reconstruction works, consider a biphase modulated signal $m(t) \sin \omega t$, where $m(t)$ is $+1$ and -1 with equal probability at the input to the squarer. At the output, $(\sin \omega t)^2$ equals $1/2 - 1/2 \cos 2 \omega t$. The second term is a "line" at twice the input frequency. To maximize the signal-to-noise ratio out of the squarer at low input signal-to-noise ratios, the squarer is preceded by a filter matched to one chip (1.25 msec, see Fig. 2) of the modulation. In addition to the desired "line" and noise, the squarer output also contains a pair of weaker lines ±800 Hz from the desired lines. Circuitry was included to prevent locking on these lines. Further discussion of carrier reconstruction is given in Appendix B.

Acquisition of beacon RF frequency and phase proceeds in three steps. The receiver (a) scans the frequency uncertainty region in search of a reconstructed carrier, (b) phase locks on the reconstructed carrier of the detected signal, and (c) tests the acquired signal for biphase modulation (i.e., for very small real carrier).

a. Frequency Search

Figure 3 shows the essential elements of the frequency search operation. In response to the search control input, a voltage controlled crystal oscillator (VCXO) is tuned continuously over the frequency uncertainty region. The mixer output is passed through the matched filter centered at the IF frequency ω_{IF} and is then squared to reconstruct the carrier. The cascaded narrowband
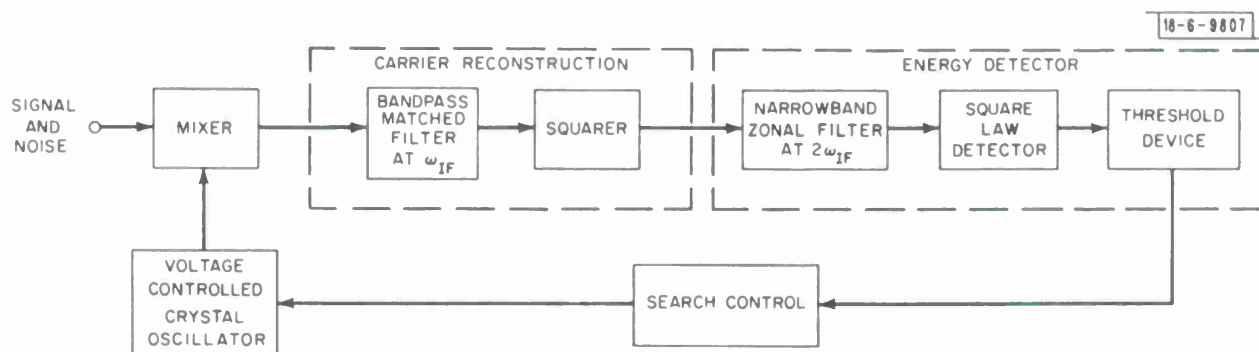
Fig. 3. Essential elements of frequency search.

zonal filter, squarer, and threshold stage constitute a detector which examines the energy in the vicinity of $2\omega_{IF}$ and stops the search on sensing a "line" of sufficient magnitude.

The equivalent voltage-controlled crystal oscillator (VCXO) sweep rate referred to the satellite beacon frequency is 37 Hz/sec, and the narrowband first-order filter has a 3-db bandwidth of 3.2 Hz. For these parameters a biphase signal with a P_r/N_o of 30 db (Hz) is detected with a probability greater than 0.9. The probability of detection for a given sweep rate is very sensitive to P_r/N_o. In particular, a decrease in P_r/N_o to 28 db (Hz) results in a probability of detection less than 0.1. These parameters determine the minimum P_r/N_o for successful acquisition. Further discussion of the frequency acquisition scheme is given in Appendix C.

In the event of a fade, the receiver waits about 8 sec, which is considerably longer than the duration of a normal multipath fade experienced by an aircraft terminal. If the line is not redetected during that interval, it is assumed that the link doppler has changed sufficiently to shift the line out of the filter passband, and the VCXO sweep is reactivated.

b. Phase Lock

A second-order phase-locked loop (Fig. 4) is enabled when the frequency search detector announces the presence of a line within the narrowband zonal filter. If this loop does not pull in and lock within 8 sec after line detection, the search control reactivates the frequency search.

The loop is designed to have a noise bandwidth of 10 Hz with good transient response characteristics when the P_r/N_o of the beacon signal is 27 db (Hz) and should be able to maintain phase lock in the presence of a 10-Hz/sec drift at that P_r/N_o. Appendix D treats the loop performance in detail.

The phase lock detector is also included in Fig. 4. When the reconstructed carrier is coherently demodulated, the lock detector lowpass filter provides a predictable DC output. Phase lock is assumed if this filter output exceeds threshold, and the inclusion of a fixed output delay enables the detector to tolerate short fades and/or occasional loop cycle-slipping without re-initiating a search.
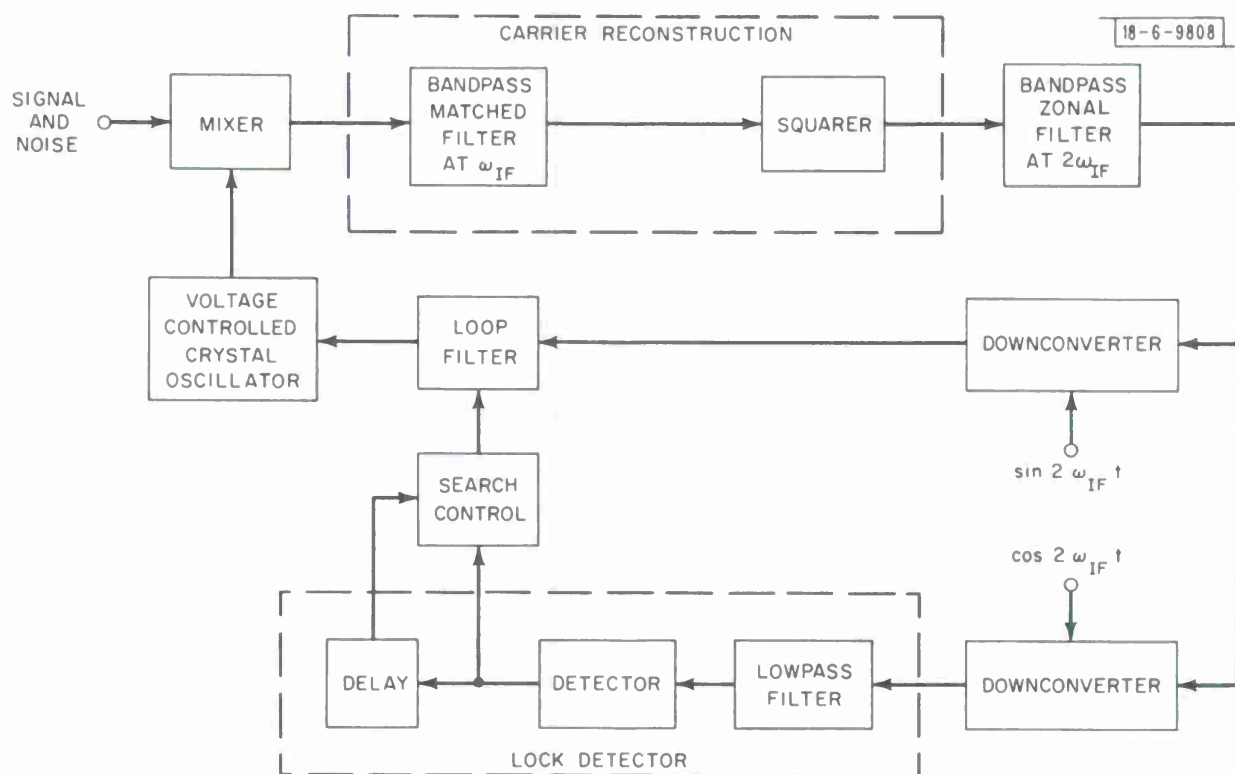
10

Fig. 4.   Conceptual diagram of phase-locked loop and lock detector.

A brief analysis of this unconventional detector is also given in Appendix D.

Phase locking to the reconstructed carrier results in a 180° phase ambiguity relative to the actual carrier phase [i.e., $(-1)^2$ is the same as $(+1)^2$]. The receiver logic is arranged to prevent any difficulty due to this ambiguity.

In the event of loss of phase lock, all other operations are inhibited.   If the signal is not recovered within about 8 sec, it is assumed that changing link doppler has shifted the received signal out of the pull-in range of the phase-locked loop, and the frequency search is restarted.

c.   Carrier Test

The $2\omega_{IF}$ frequency component at the squarer output may arise either from a biphase modulated signal such as the beacon or from a carrier, unmodulated or amplitude modulated.   One distinguishing feature of the biphase modulated signal is the zero or very small carrier component (i.e., component at ω_{IF})

11

in the unsquared signal. To identify and quickly reject any "false locks," i.e., phase lock on signals other than the desired beacon signal, the receiver tests for a carrier component at ω_{IF} immediately after phase lock is established at $2\omega_{IF}$. This is accomplished by the addition of a downconverter, lowpass filter, and amplitude detector at the output of the bandpass matched filter used in the carrier reconstruction circuit. If this line detector at ω_{IF} detects a carrier component larger than that which could arise from the beacon signal, the search control reactivates the frequency search. If the phase detector output remains below threshold, acquisition of a valid signal is tentatively assumed, and the receiver proceeds to acquire timing synchronization.

2. Time Acquisition

The second part of the acquisition process, that of aligning local framing and sequence replicas with their received signal counterparts, begins when phase lock is established. As the time demodulator coarse-aligns framing and the five binary sequences one by one, a parallel fine-align operation resolves the error in the composite timing pattern (framing plus aligned sequences) to a small final value.

Time acquisition and tracking proceed only while the undelayed phase-lock detector indicates phase lock. Because of the 180° ambiguity in the reconstituted carrier relative to actual carrier phase, the receiver must test, and if necessary correct, the polarity of the framing signal when phase lock is re-established after loss of lock. For convenience, before resuming an interrupted search, the receiver also checks all sequences aligned prior to loss of lock. Since this checking is quite rapid, acquisition in most fading environments does not require substantially more time than in nonfading environments with the same direct path signal strength.

a. Framing Acquisition

The framing signal is a periodic sequence of 1.25-msec pulses that occupies the first position within each 10-msec frame. Framing acquisition is accomplished by successively cross-correlating the received signal, coherently

12

demodulated to lowpass, with all possible time shifts of a locally generated replica of the framing signal (Fig. 5). The local signal is stepped in increments of one-half pulse period (625 μsec), so that the maximum misalignment with the received signal will ordinarily be one-quarter of a pulse period. However, because of the 180° ambiguity in carrier phase acquisition, the polarity and time offsets of the local replica are equally significant. Accordingly, by adopting an interlaced invert/shift search, a signal may be found by examining 32 positions, at most.

Fig. 5. Sequential coarse time-alignment.
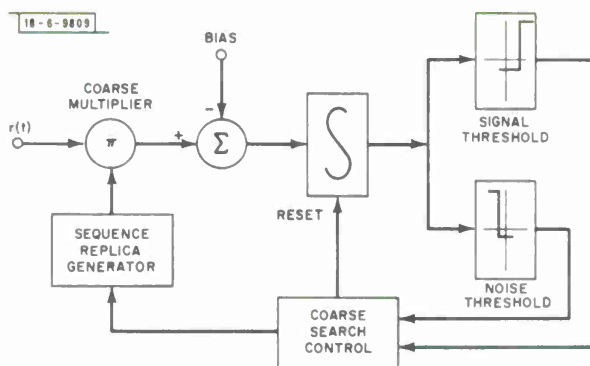
The coarse timing section uses a sequential search to minimize average acquisition time. The integrator output (Fig. 5) is examined until it crosses one of two thresholds, corresponding to either "signal present" or "no signal present" (i.e., misalignment).

If no framing signal is acquired within a set number of search cycles following frequency lock, the receiver assumes it has locked on a false signal and resumes the frequency search. Similar action is taken if any of the timing sequences cannot be acquired after several attempts.

b. Sequence Acquisition

As soon as the framing signal is detected at a particular time offset, the coarse-align loop begins the task of aligning the five binary sequences. The sequence acquisition procedure is much like that indicated in Fig. 5, except that with framing aligned, a 180° ambiguity no longer exists, and timing is slewed in one-frame increments. Sequences are acquired one at a time,

13

eliminating the need for more than one correlation-detection system. The acquisition procedure is analyzed in Appendix E.

c. Fine Time Alignment

The fine-align, modified delay-lock loop is shown in Fig. 6, where the demodulated input signal r(t) is multiplied by phased versions of the local composite replica. A discrete correction signal is generated by correlating one-half pulse period lead and lag replicas with r(t), integrating the difference
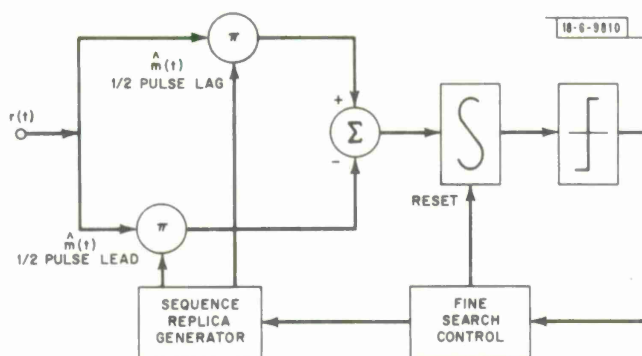

Fig. 6. Fine time-alignment delay-lock loop.

of the products, and measuring the error at the threshold detector output. Utilizing a fixed 5-μsec correction increment, the fine-align servo loop reduces receiver timebase offset to a small residual jitter. In response to changes in polarity of the error, the initial slew rate of 25 corrections/sec is first switched to an intermediate 5 corrections/sec rate; then to a final rate of 1 correction/sec. This 3-speed scheme reduces loop pull-in time without compromising steady-state performance.

As each sequence is detected by the coarse-alignment circuitry, it is incorporated into the reference signal of the time-locked loop (Fig. 6) along with the framing signal. This makes more energy available for loop operation, increasing the effective signal-to-noise-density ratio, and because of the complex nature of the timing sequences makes the loop less susceptible to interference.

The time loop tracking performance has a standard deviation of about 10 μsec with a received beacon P_r/N_o of 30 db (Hz). At higher signal-to-noise-density ratios the fine time error is limited by the minimum step size.

14

Corrections are made each second so the maximum rate of change of time delay that could be tracked is $5\,\mu\mathrm{sec/sec}$.

B. Monitor Mode

Upon completing synchronization of framing and all sequences, the receiver automatically switches from the acquire mode to the monitor mode. The local replica of slots S1 through S6 of the beacon modulation, having been synchronized with the beacon signal, now multiplies the received signal to remove the latter's modulation. The multiplier output is zeroed during slots S7 and S8. The resulting demodulated carrier replaces the reconstructed carrier, permitting tracking at received P_r/N_o's nearly 10 db below the minimum using the reconstructed carrier.

The receiver continually checks the alignment status of each slot within the beacon timing pattern. In the event that a misalignment is detected, the receiver provides an external error status indication, and attempts to realign the sequence in error. Once the sequence is properly realigned, the test is repeated with the next sequence. Misaligned sequences, when detected, are removed from the fine time loop reference.

In the event of loss of phase lock, all timebase and sequence shifting is inhibited. If the signal is not recovered within about 8 sec, the receiver reverts to a search mode, identical to the acquire mode, except that the local replica is still used to provide a demodulator reference. If this search does not reacquire the signal within about one minute, it is assumed that the local timebase replica may have drifted out of alignment with the received signal. Therefore the receiver reverts to the acquire mode by replacing the local reference demodulator output with the squarer (reconstructed carrier) output. The logic is arranged so that the timebase is maintained at the most recent known alignment to minimize reacquisition time.

C. Auxiliary Functions

This part describes additions to the receiver that increase test convenience and operational utility at nominal component cost.

1. Telemetry Detector

Slot S8 contains telemetry information in standard bit-to-bit differential format. Since suitable timing signals were available from the sequence synchronization scheme, an integrator, a threshold device, and a very simple decoder were added to provide telemetry output. Because the timing reference is essentially perfect in this application, the achieved telemetry error rate performance is essentially identical to that of a perfect detector operating at the same P_r/N_o.

2. Signal-to-Noise and Frequency Indicators

The VCXO control voltage is connected to a front panel meter to give an indication of frequency. Because all mixer reference signals are derived from the VCXO (Appendix A), calibration of this meter provides a highly accurate frequency measurement.

The output of the phase-lock detector narrowband filter is applied to a front panel meter to indicate the received signal-to-noise-density ratio. The meter indication is actually an indication of the total power passed by the narrowband filter centered on the received carrier (reconstructed carrier, in the acquire mode), normalized by the total power in the IF bandwidth (about 4 kHz) of the receiver. Assuming the only interference is Gaussian noise, the meter can be calibrated directly in P_r/N_o. The resulting display can be read to within 1 db for P_r/N_o's less than 38 db (Hz).

3. Beacon Timing Simulator

A beacon timing generator is included within the time demodulator section. This permits a baseband self-check of receiver timing acquisition and tracking, and also provides a convenient modulation source for synthesizing a UHF beacon test signal.

IV. RECEIVER PERFORMANCE

A breadboard receiver, tested extensively to verify basic design ideas, was first used for a preflight check of LES-5. During launch, it operated

16

with the 30-ft-diameter paraboloidal antenna atop B Building, Lincoln Laboratory, Lexington, Massachusetts, to monitor telemetry data contained in the beacon signal.

Based on experience with the breadboard receiver, a second generation unit was built (Appendix A). This receiver received LES-6 signals on several test flights,[*] and has monitored the LES-6 beacon from the 30-ft antenna in Lexington, Mass., as well as via a 10 db-gain helix.

Several copies of the second generation receiver were built by a private contractor. Two of them have been tested sufficiently to establish their proper operation. Test results agree with theoretical predictions.

Receiver performance is illustrated by three tests made on one of the copies. For the tests, a simulated beacon signal was added to a known noise source and fed to the receiver. Calibration accuracy of the resultant P_r/N_o is believed to have been better than 1 db.

A. Acquisition

Over a range of P_r/N_o values, ten or more trials were made during which the receiver was reset to the acquire mode and allowed one sweep through the frequency uncertainty region. Results (i.e., acquisition success or failure) were recorded for each trial. Three distinct sets of results were observed. While acquisition was always possible at high P_r/N_o's and never possible at low P_r/N_o's, there existed an intermediate region [P_r/N_o = 29 db (Hz)] within which acquisition was sometimes possible. Twenty-five trials were made at this intermediate signal-to-noise density ratio. The percentage of first-sweep acquisition is shown in Fig. 7. These results are in good agreement with the theory (Appendix C).

B. Dropout

To test receiver performance at P_r/N_o's below the initial acquisition threshold, the receiver was permitted to complete acquisition at a P_r/N_o above threshold. Then the P_r/N_o was lowered in 1-db steps, holding at each
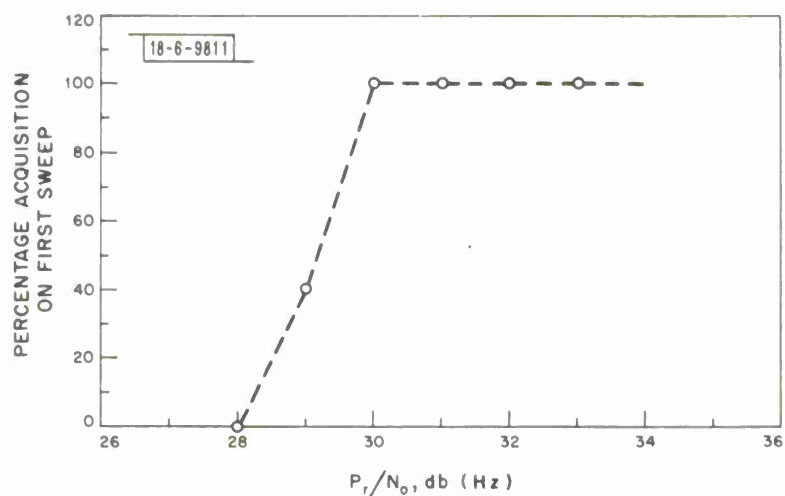
---

* AFSC C-135 aircraft.

17

Fig. 7. Receiver acquisition performance based on 10 runs at each P_r/N_o, except 25 runs at $P_r/N_o = 29$ db (Hz).
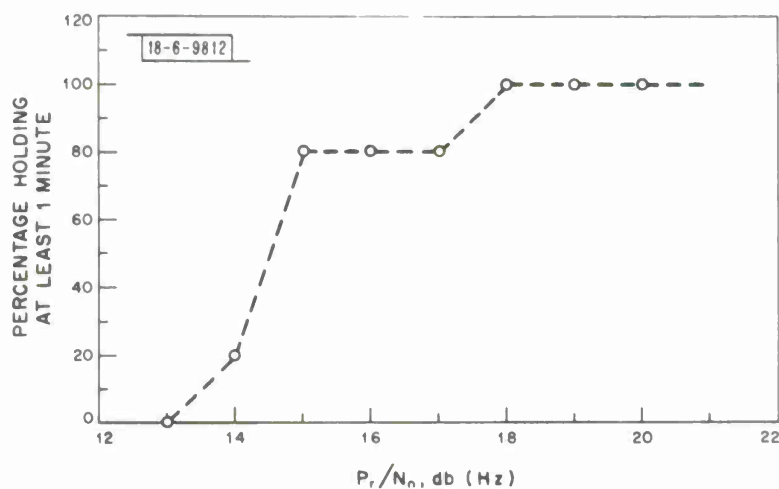

Fig. 8. Receiver dropout performance based on 5 runs holding at least one minute at indicated P_r/N_o.

value for about one minute to see if the receiver maintained reliable synchronization. The test was repeated five times (Fig. 8). In reasonable agreement with theoretical predictions, the receiver never lost synchronization at P_r/N_o's of 18 db (Hz) or greater.

C.   Time Jitter

Synchronization was established initially at a P_r/N_o of 50 db (Hz). Timing reference waveforms from the beacon simulator and receiver demodulator were compared on an oscilloscope for about two minutes. The peak time jitter observed was recorded, the P_r/N_o was reduced by 2 db, and the experiment repeated. Observations (Fig. 9) were made down to a P_r/N_o of 16 db (Hz). These results are in reasonable agreement with the analysis in Appendix F.
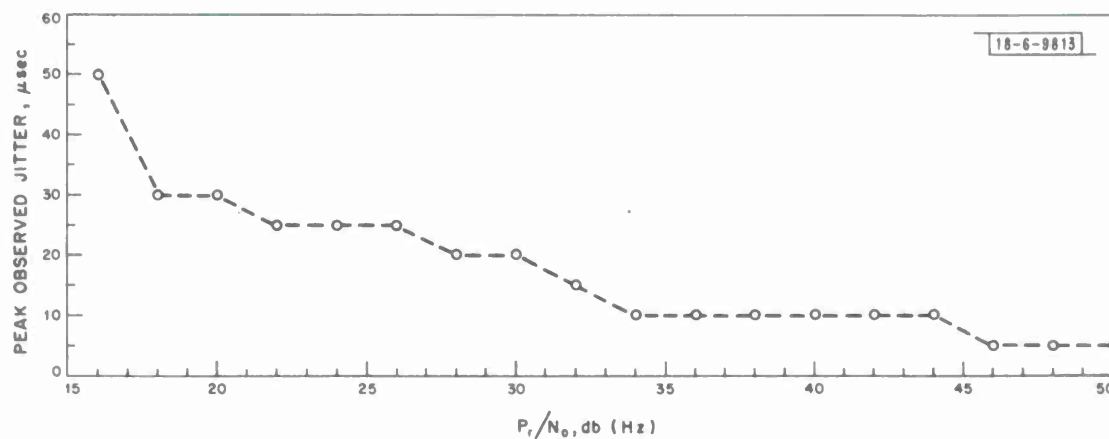

Fig. 9.   Receiver time tracking jitter based on a two-minute observation at each P_r/N_o.

APPENDIX A
REALIZATION

The following discussion outlines the operating algorithm for the LES-5 automatic beacon receiver, and develops the baseband frequency search realization. The overall receiver is discussed in terms of its RF, frequency demodulator, and time demodulator sections. Salient characteristics and design features of each section are given.

1. GENERAL

The overall receiver operating algorithm, as described within the report, is presented in the flow chart (Fig. A-1). Operation is discussed in terms of ACQUIRE and MONITOR modes. Whenever the system is in ACQUIRE mode, the receiver uses a matched filter-squarer scheme in conjunction with a second-order control loop to phase-lock on the reconstructed carrier of the detected signal. After validity of the detected signal is confirmed, the local timing replica (framing plus sequences) is aligned quickly with the detected satellite modulation by slewing the local timing reference. On completion of timing synchronization, the receiver switches automatically to the MONITOR mode. At this time, the demodulated carrier replaces the reconstructed carrier within the phase-locked loop, and the alignment status of each slot within the beacon timing pattern is checked continually. Provision is made for the automatic restoration of frequency and time sync after a temporary loss of RF signal.

The essential elements of the frequency search and the phase-locked loop have thus far been discussed in terms of their bandpass representations (Figs. 3 and 4). However, the actual frequency demodulation section (i. e., frequency search, carrier phase-lock; signal recognition) was realized at baseband. The following discussion presents the evolution of a baseband frequency search model, including detectors, and cites the reasoning behind each choice.

Referring to the bandpass frequency search model (Fig. 3), the cascaded narrowband zonal filter, squarer, and threshold stage constitute a detector of energy at twice the intermediate frequency, $2\omega_{IF}$. Because narrowband filters
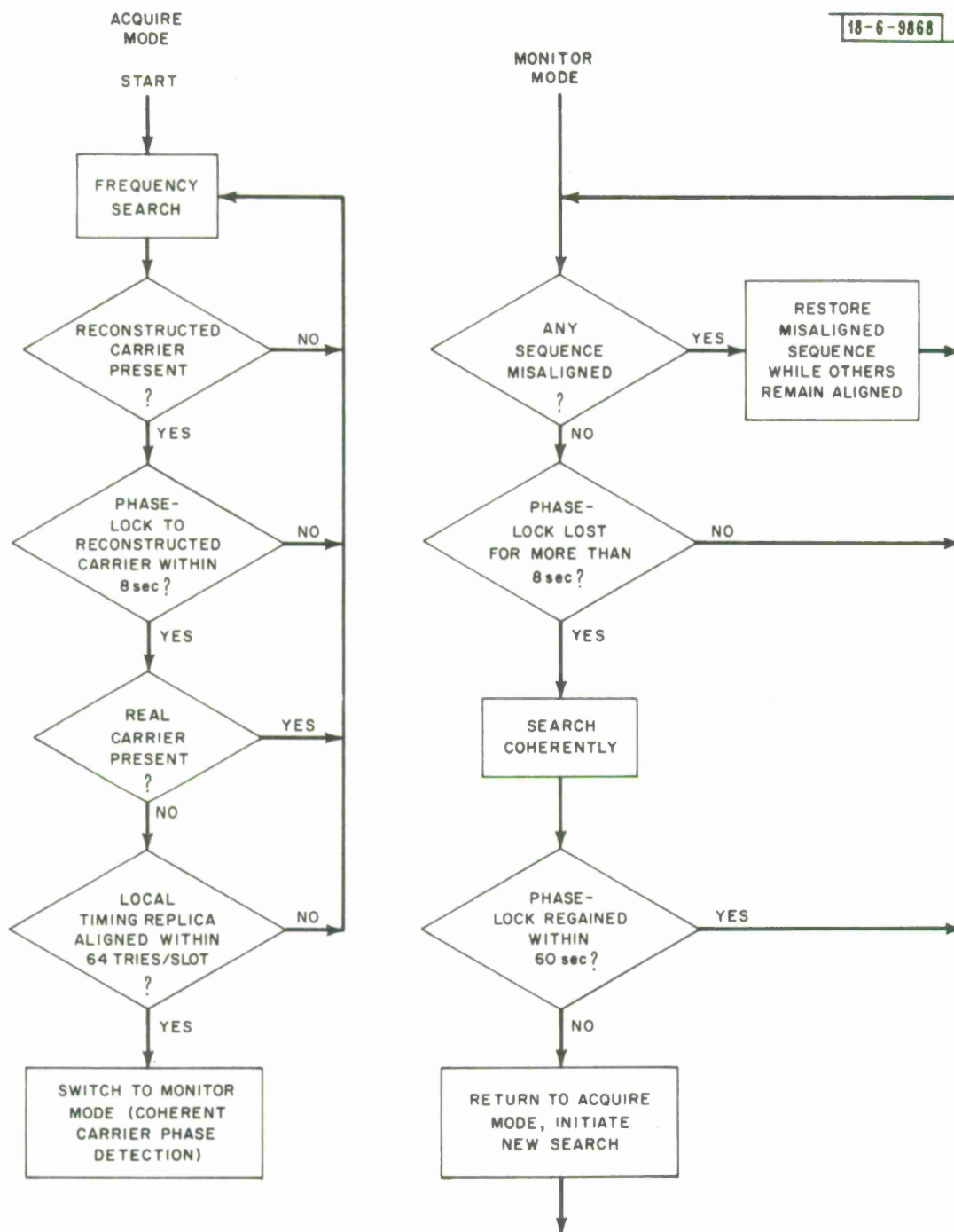
21

Fig. A-1. Beacon receiver operating algorithm.

are more easily realized at lowpass,[A1] it is useful to implement the energy detector as shown in Fig. A-2. Whenever energy is sensed within the narrow band of the detector, the search is interrupted and the control loop attempts to phase-lock on the reconstructed carrier.

The conceptual diagram of the second-order control loop, together with phase-lock detector, was originally presented in Fig. 4. The baseband equivalent model of the loop is shown in Fig. A-3. When beacon carrier phase-lock is achieved, the lock detector LPF output exceeds threshold, and announces phase lock to the search control.

To identify and reject phase-locks on signals other than the correct beacon signal, the system tests for a carrier component at ω_{IF}. If a carrier component is detected that could not possibly have arisen from a valid beacon signal, the carrier detector (Fig. A-3) reactivates the frequency search.

Recalling that narrowband filters are more easily realizable at lowpass, that part of the demodulation system up to points A and B can be replaced with a two-phase synchronous scheme described by Costas.[A2] A brief trigonometric exercise verifies equivalence of the squaring and Costas schemes. Figure A-4 shows the final squaring mode configuration, including energy, phase-lock, and carrier detectors. Absolute value circuits have been substituted for all squarers used in baseband signal processing. The approximation to the square-law characteristic is a good one at the specific signal-plus-noise levels of interest.

Earlier reference was made to the use of a modified frequency loop configuration after time synchronization is achieved. For coherent operation, the loop of Fig. A-5 replaces the Costas loop, and permits narrowband tracking at signal-to-noise-density ratios several db below minimum for squaring mode. Note that the loop error signal is now derived by cross correlation of the quadrature baseband signal with the aligned local timing replica, and that the carrier detector is no longer used.

Figures A-4 and A-5, respectively, present the receiver configuration for (a) frequency acquisition and carrier phase lock in ACQUIRE (squaring) mode, and (b) coherent narrowband tracking in MONITOR (coherent) mode. From a hardware standpoint, it is more convenient to consider the receiver as a system
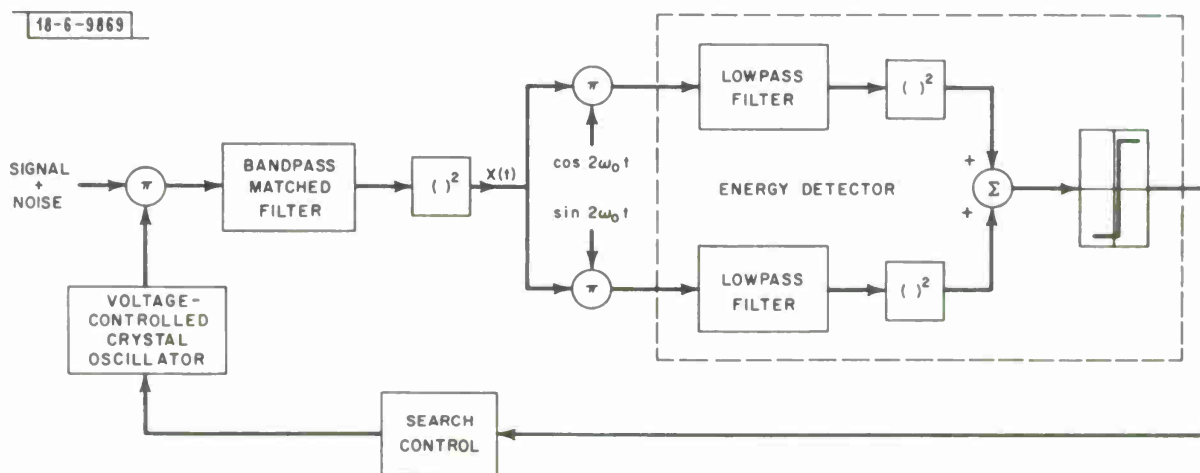
Fig. A-2.   Essential elements of frequency search with lowpass energy detector realization.
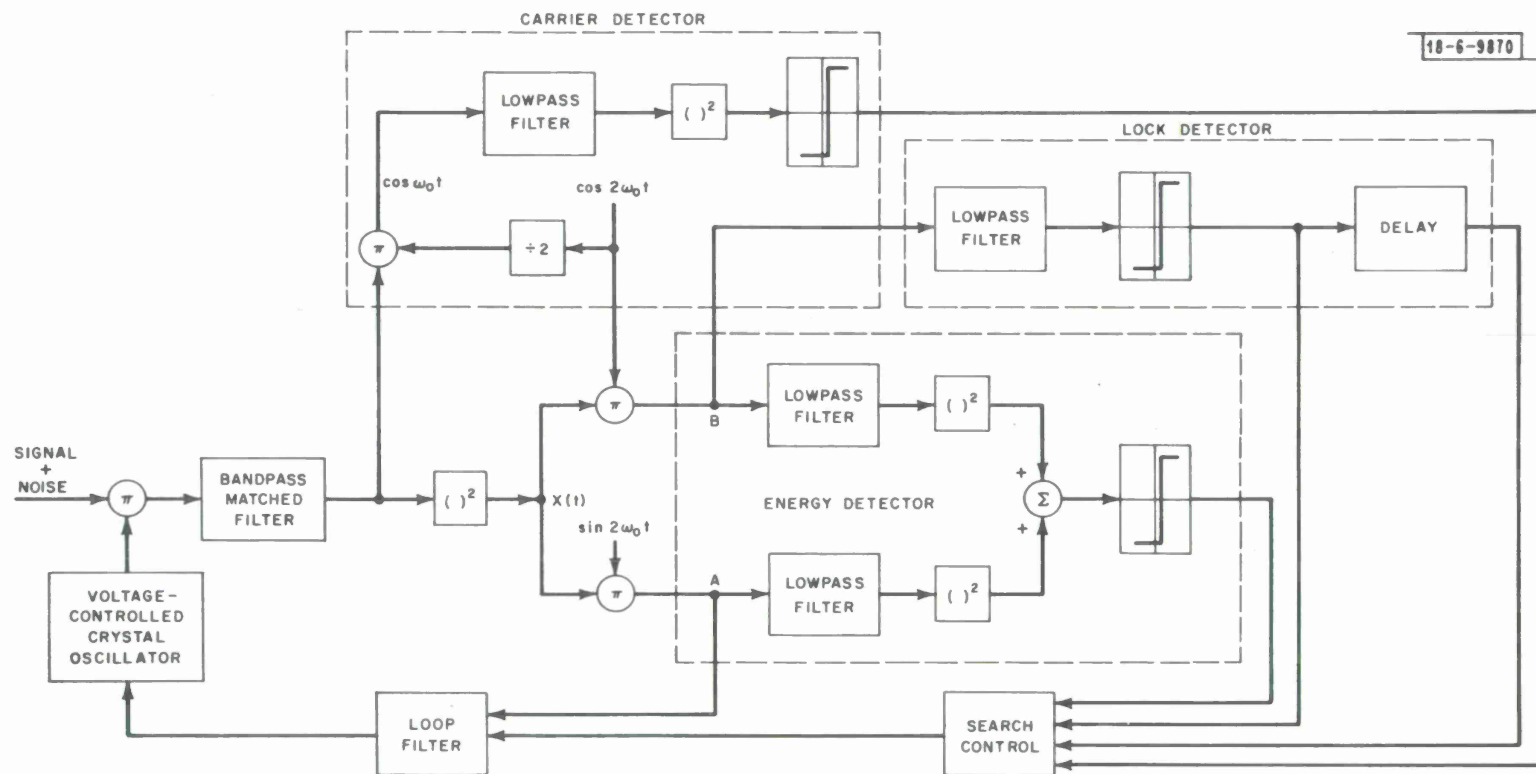
18-6-9870

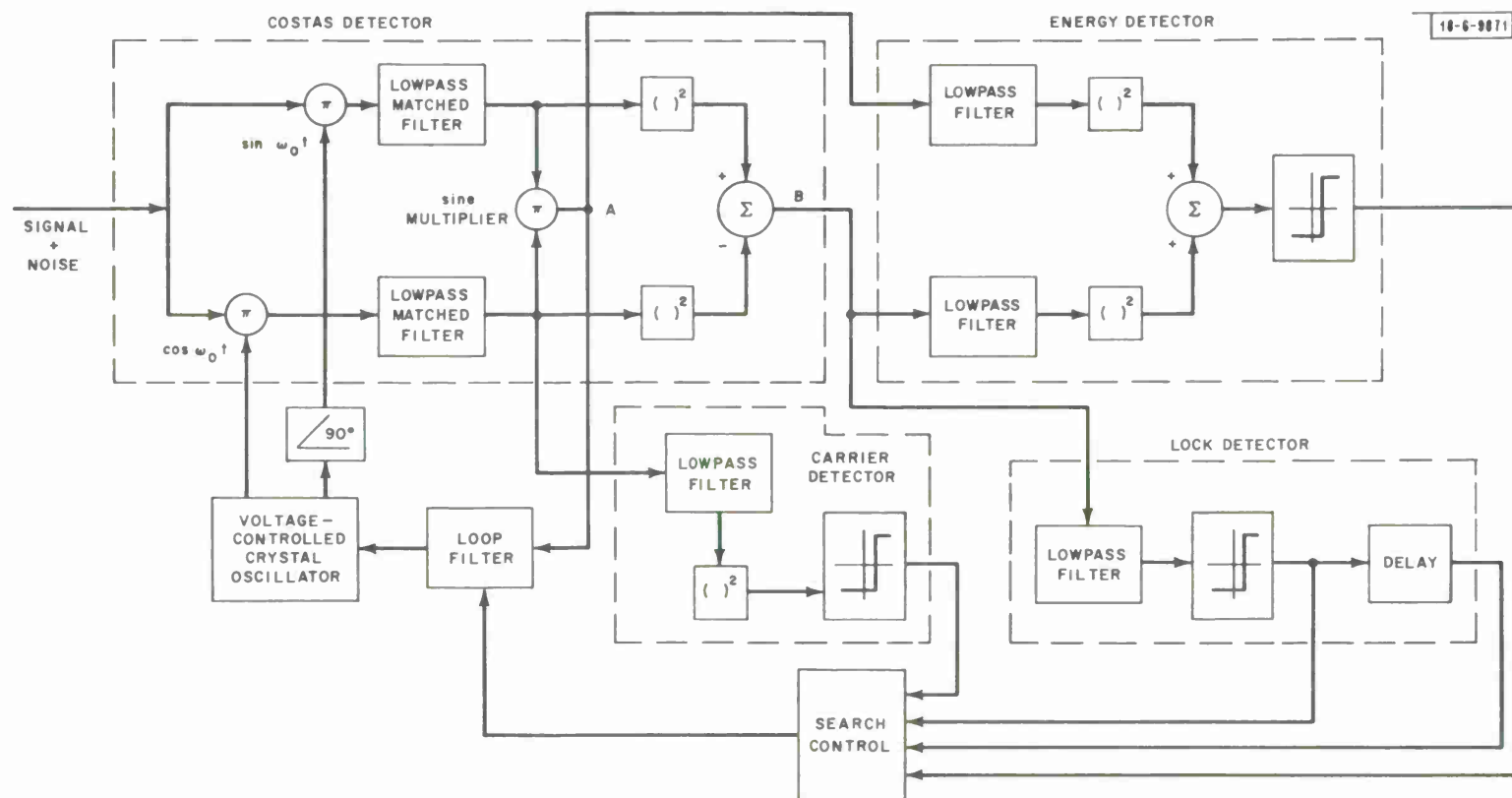Fig. A-3.   Phase-locked loop with energy, carrier, and lock detectors.

Fig. A-4. Costas' realization of frequency loop with energy, lock, and carrier detectors.
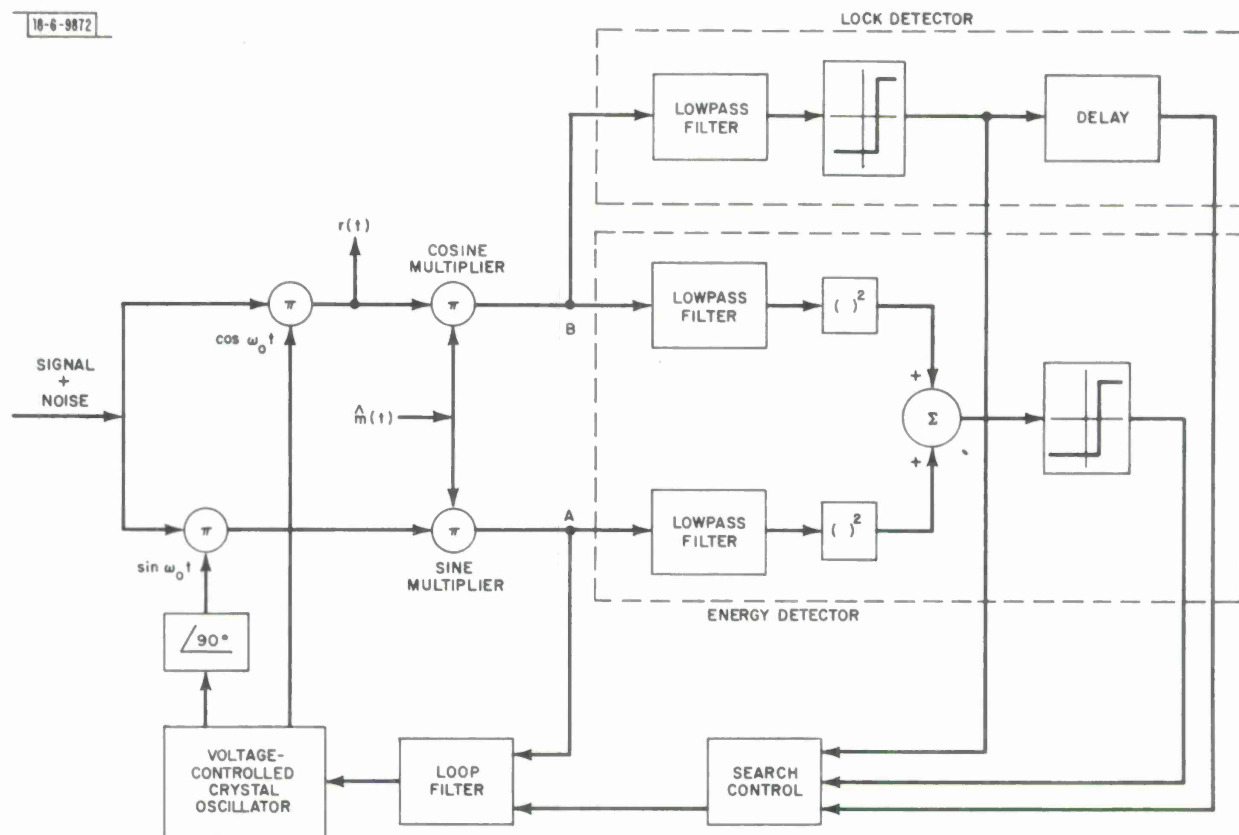
Fig. A-5. Frequency loop configuration for coherent mode.

composed of three sections; viz., an RF section, a frequency demodulator, and a time demodulator. Physically, each section is comprised of one or more modules (Fig. A-6).

2. RF SECTION

The basic function of the RF section is to translate, amplify, and convert incoming beacon signals to in-phase and quadrature lowpass signals for the frequency and time demodulators. The RF block diagram is shown in Fig. A-7. To obtain good dynamic range, overload, and out-of-band rejection character- istics, selectivity-determining components were preceded by the minimum gain possible without compromising sensitivity. Specification and maintenance of conversion signal frequency and phase characteristics were simplified by deriving all frequencies from a single oscillator. Other design features of note are:

a. Doubly balanced mixers to provide wide dynamic range.

b. A first mixer injection signal derived by a divide-and- phase-lock stalo programmable in 100-kHz steps over a 1-MHz range.

c. A second mixer injection signal derived by a divide-and- phase-lock stalo programmable in 5-kHz steps over a 100-kHz range. This feature was included to permit op- eration with future satellites.

d. A second IF amplifier having very wide dynamic range and high gain with an internal constant average envelope AGC. This IF amplifier offers somewhat better perform- ance than would be possible with a hard limiting IF am- plifier under certain conditions.

e. Balanced high-level downconverters to provide fractional- volt baseband signals with millivolt DC offsets.

3. FREQUENCY DEMODULATOR

The frequency demodulator section accepts quadrature baseband input signals from the RF section, and controls the frequency search and subsequent narrowband tracking of the beacon carrier at low signal-to-noise-density ratios. The frequency demodulator, with both squaring and coherent configurations denoted, is shown in Fig. A-8. Conventional digital timers within the search
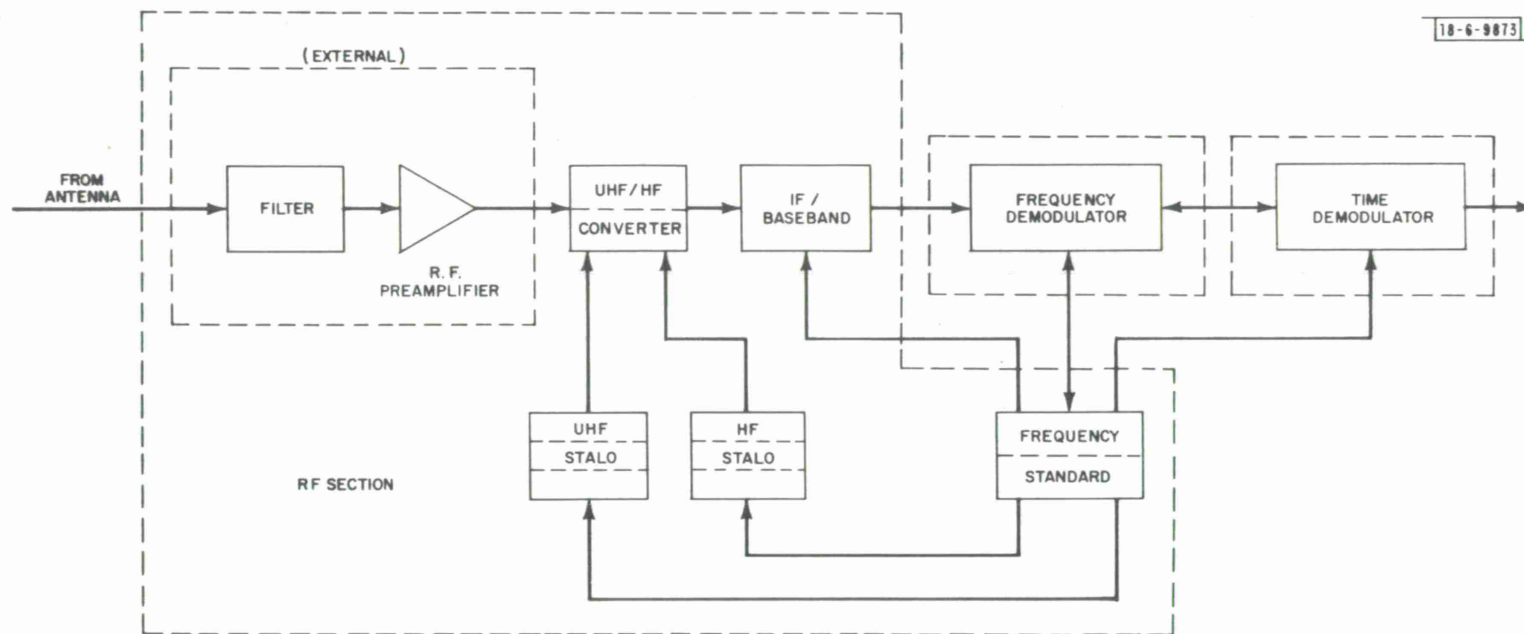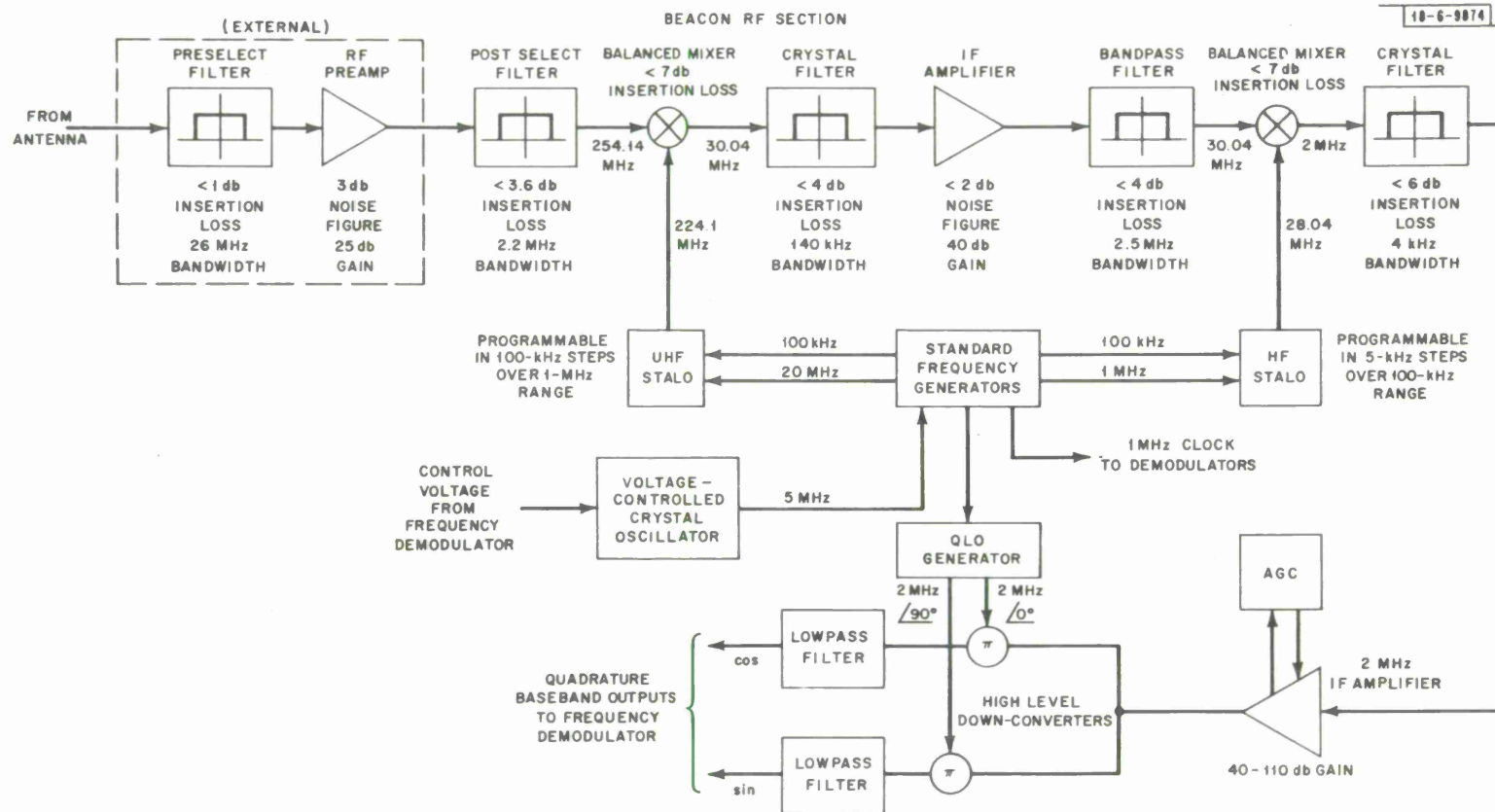
Fig. A-6.   Beacon receiver block diagram.

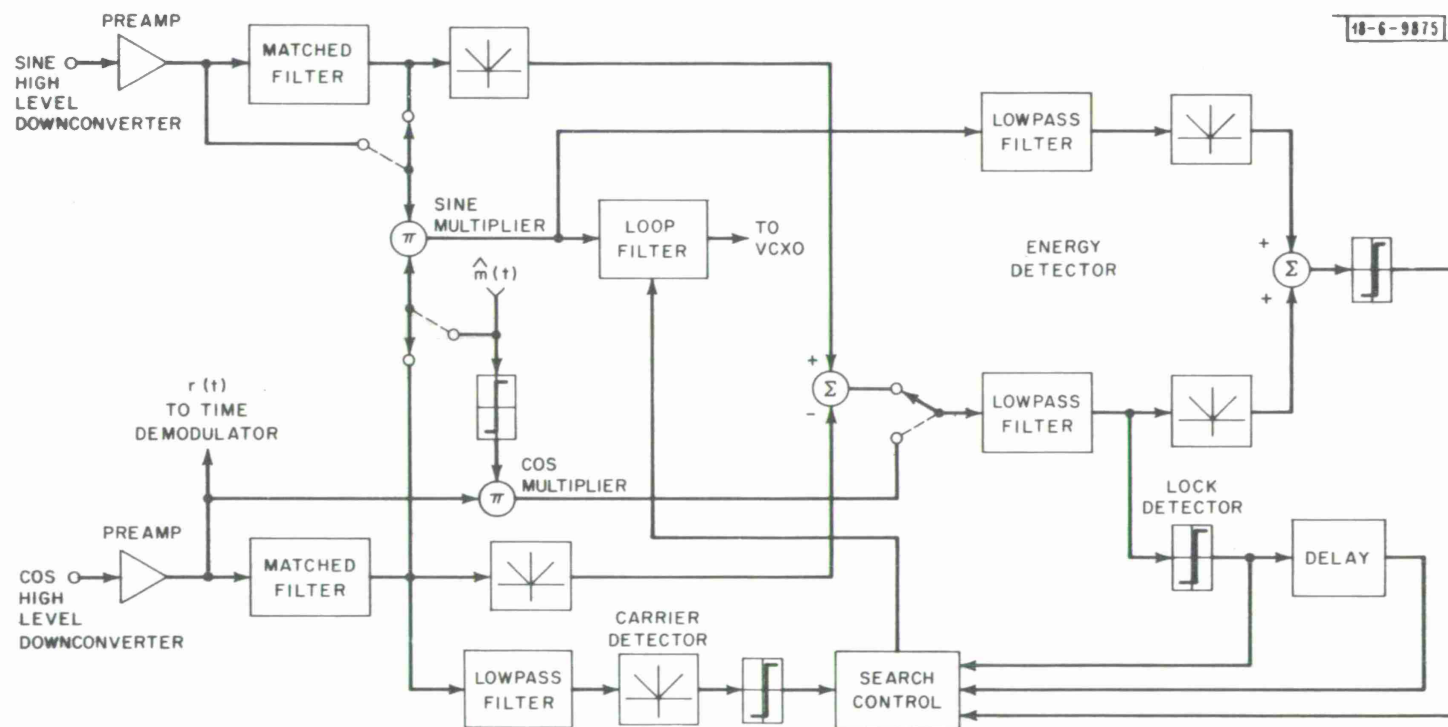Fig. A-7.   UHF beacon receiver RF section (LES-6 configuration).

Fig. A-8.   Frequency demodulator section shown in ( )^2 mode.   Move switches for coherent mode.

control operate in response to detector inputs to provide appropriate delays for phase lock, signal fades, and coherent search (Fig. A-1). Noteworthy hardware features are:

   a. Low leakage FET switching between squaring and coherent configurations.

   b. Absolute value circuits used as approximations to squarers.

   c. An active loop filter having a limited and resettable output (VCXO control) with negligible drift.

   d. Baseband multipliers realized via a "half linear" scheme in which an analog multiplicand and a digital multiplier are processed using logic-driven FET switches with an integrated circuit operational amplifier.

4. TIME DEMODULATOR

The time demodulator section accepts the in-phase baseband signal from the frequency demodulator, $r(t)$, and uses coherent decorrelation techniques to align a local timing replica with the received satellite timing pattern.

As outlined earlier in this report, time synchronization is carried out in parallel by coarse and fine control loops. Simplified conceptual diagrams of the coarse and fine loops, plus the telemetry detector, are shown in Fig. A-9. Salient receiver features associated with the time demodulator are:

   a. The ability to recognize unacceptable signals, and to command a resumption of the frequency search.

   b. Automatic monitoring of timing sync status, with time flywheel capability in the presence of signal fades.

   c. Built-in self-check circuitry.
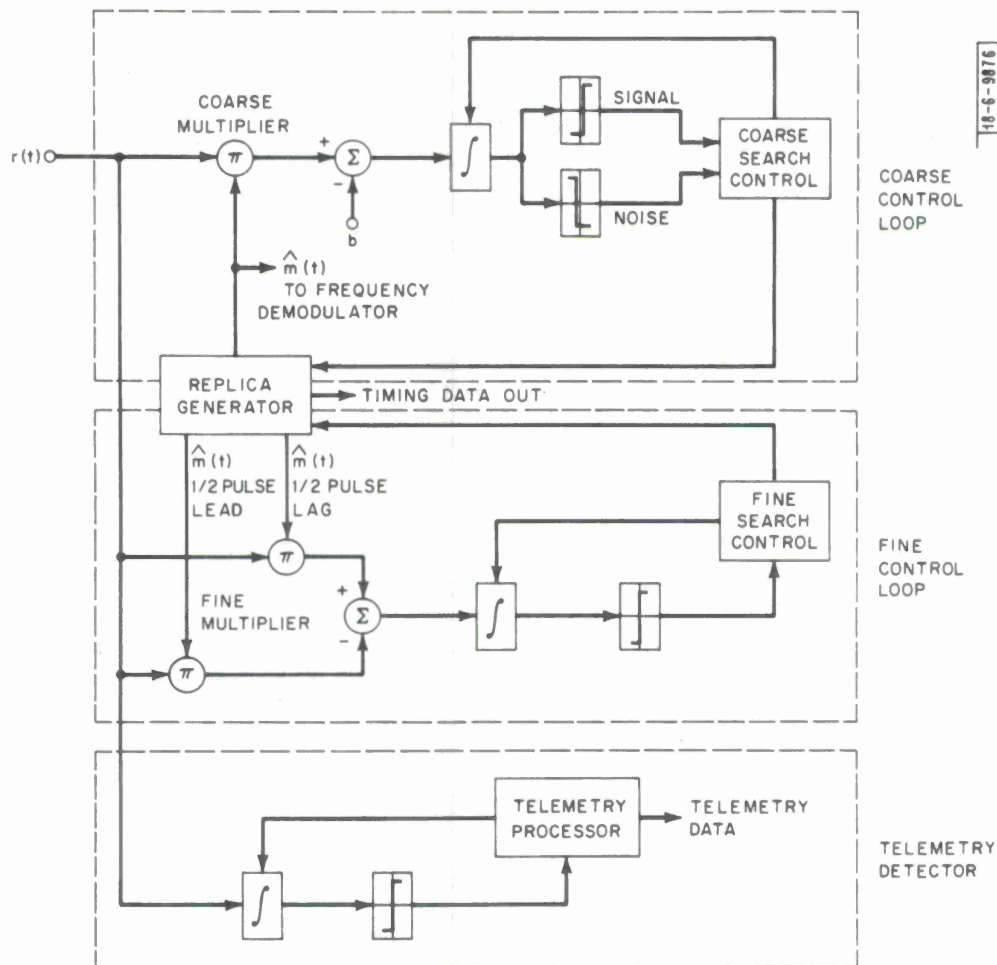
   d. Serial and parallel timing data outputs.

32

Fig. A-9. Time demodulator functional diagram.

APPENDIX B
CARRIER RECONSTRUCTION

The biphase beacon signal of average power P_r may be written

$$\sqrt{2P_r}\, m(t)\cos \omega t$$

where $m(t) = \pm 1$. The probability that $m(t)$ is $+1$ is almost $1/2$, so $\overline{m}(t)$ is approximately zero and the real carrier component of the beacon signal is quite small. A conventional technique for generating a coherent reference carrier is to pass the biphase signal through a square law device.

This appendix describes some aspects of this carrier reconstruction technique that are not well known, but which are useful in system design.

The beacon signal is received in the presence of additive white Gaussian noise of real (single-sided) spectral density N_o. Therefore, the received signal plus noise may be written as

$$[\sqrt{2P_r}\, m(t) + n_1(t)]\ \cos \omega_c t + n_2(t)\sin \omega_c t \quad ,$$

where $n_1(t)$ and $n_2(t)$ are lowpass Gaussian random processes with double-sided spectral heights of N_o. The received signal plus noise is filtered and squared. With $\sim$ to denote "filtered," the double frequency output of the squarer is

$$\left[P_r \widetilde{m}^2(t) + \sqrt{2P_r}\, \widetilde{m}(t)\, \widetilde{n}_1(t) + \frac{\widetilde{n}_1^2(t) - \widetilde{n}_2^2(t)}{2} \right] \cos 2\omega_c t$$

$$+ \ [\sqrt{2P_r}\, \widetilde{m}(t)\, \widetilde{n}_2(t) + \widetilde{n}_1(t)\, \widetilde{n}_2(t)]\, \sin 2\omega_c t \quad ,$$

The desired "line" is $P_r \overline{m^2(t)}\cos 2\omega_c t$; the remainder of the output is a sum of spurious signals and noise.

1. Optimum Filtering

Since very narrowband processing techniques must be used for operation at low P_r/N_o's, a reasonable design approach is to precede the squarer with

a filter that maximizes the squarer output ratio of line power to the equivalent noise density near the line.   Let H(s) be the equivalent baseband transfer function of the filter.   Ignoring the self-noise term

$$P_r \left[\tilde{m}^2(t) - \overline{m^2(t)} \right] \cos \omega_c t \quad ,$$

a straightforward calculation shows that

$$|H(s)|^2 = (G \sin c^2 \omega T/2)/(1 + 2E_c/N_o \sin c^2 \omega T/2)$$

where

$\quad\quad$ G = an arbitrary gain

$\quad\quad$ T = duration of one beacon signalling chip (1.25 msec
$\quad\quad\quad$ for LES-5 and -6)

$\quad\quad$ E_c = energy in one chip

$\quad\quad$ N_o = input noise spectral density

and $\sin c \, X \triangleq \sin X/X$.   From the form of this equation it follows that an optimum filter at low E_c/N_o is matched to a single chip of the modulation.

The corresponding squarer output signal-to-noise density ratio (P_s/N_s) is

$$(P_s/N_s)_{opt} = 1/2 \, (E_c/N_o)^2 \int_{-\infty}^{\infty} \frac{\sin c^4 \, \omega T/2}{1 + 2E_c/N_o \, \sin c^2 \, \omega T/2} \, \frac{d\omega}{2\pi} \quad .$$

An analytic expression for this integral was not obtained.   However, two upper bounds derived by simplifying the integrand are

$$(P_s/N_s)_{opt} \leqslant 1/2 \, (P_r/N_o) \, [(E_c/N_o)/(1 + 2E_c/N_o)]$$

and

$$(P_s/N_s)_{opt} \leqslant 1/3 \, (P_r/N_o) \, (E_c/N_o) \quad .$$

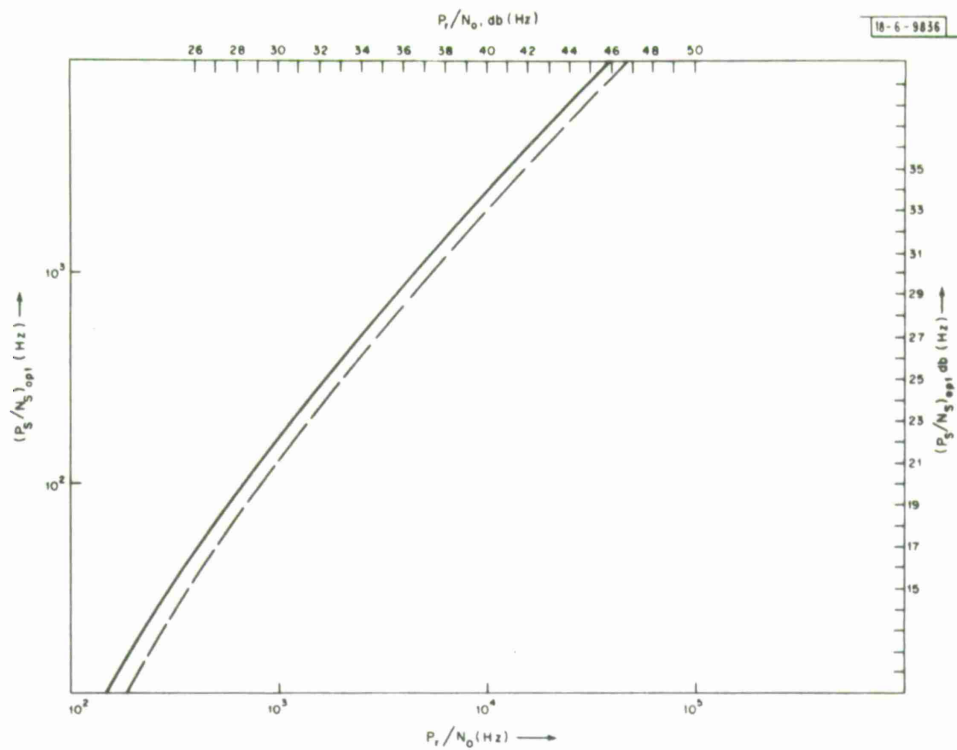The true $(P_s/N_s)_{opt}$ is asymptotically equal to the first bound for high E_c/N_o,

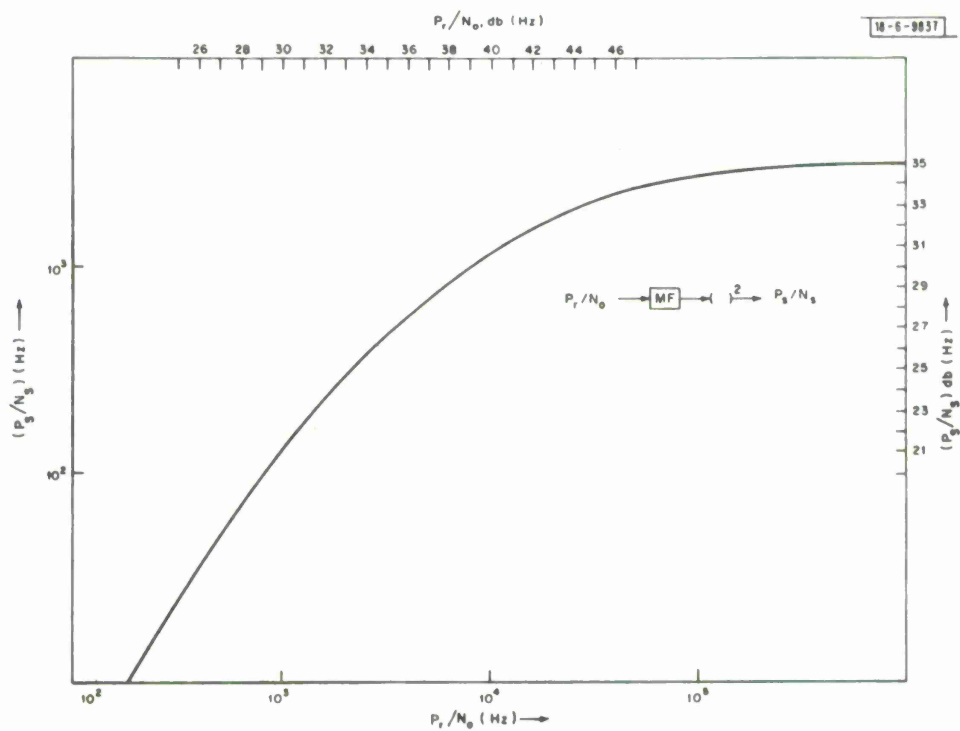Fig. B-1. Bounds on optimum filter-squarer performance (neglecting self-noise) for T = 1.25 msec.

Fig. B-2. Matched filter-squarer performance for T = 1.25 msec.

and to the second bound for low E_c/N_o. Two lower bounds, derived by application of the Schwartz inequality, are

$$(P_s/N_s)_{opt} \geqslant (27/64) \ (P_r/N_o) \ [(E_c/N_o)/(3/2 + 2E_c/N_o)]$$

and

$$(P_s/N_s)_{opt} \geqslant (1/3) \ (P_r/N_o) \ [(E_c/N_o)/1 + 33/20 \ (E_c/N_o)]$$

which are most useful at high and low E_c/N_o, respectively. For low E_c/N_o the upper and lower bounds are identical. Plots of these bounds on P_s/N_s for $T = 1.25$ msec (Fig. B-1) correspond to the LES-5 modulation. Note that the upper and lower bounds differ by 1.5 db, at most. The optimum filter, and the second upper bound on $(P_s/N_s)_{opt}$, were first given in Ref. B1.

2. Matched Filtering

Because a filter matched to one chip is fairly easy to realize, and because the optimum filter (neglecting self-noise) at low E_c/N_o is a matched filter, we evaluated the squarer output P_s/N_s, including self-noise, for such a filter over the full input range of E_c/N_o. The result is

$$P_s/N_s = 1/3 \ (P_r/N_o) \ \{(E_c/N_o)/[1 + 33/20 \ (E_c/N_o) + 1/12 \ (E_c/N_o)^2]\} \quad .$$

The three denominator terms are due to noise X noise, signal X noise, and signal X signal (self-noise), respectively. Clearly, self-noise is not important until the E_c/N_o is quite high, but it does limit the maximum P_s/N_s achievable with a matched filter.

Figure B-2 presents the foregoing expression for $T = 1.25$ msec. Comparing Fig. B-2 with Fig. B-1, the optimum filter offers very little, if any advantage for the LES-5 chip duration over the matched filter at P_r/N_o's below 35 db (Hz). Since the beacon receiver operates at these lower P_r/N_o's, the matched filter is a reasonable choice to precede the squarer.

The expression for P_s/N_s assumes that one half of the self-noise is in phase with the line, and one half is out of phase. In reality, all of the self-noise is in phase with the desired line. This distinction is not relevant when dealing with incoherent subsystems such as that used for frequency acquisition,

37

but highly accurate calculations of phase-coherent subsystems should be made with an appropriately modified expression for P_s/N_s. As noted, the self-noise is negligible compared to other noises at the P_r/N_o's of primary interest in the beacon receiver.

3. Sidebands

The square of the filtered modulation signal, $\tilde{m}^2(t)$, contains weak sidebands at multiples of $1/T$ Hz away from the desired dominant line, in addition to the self-noise. To determine the strength of these sidebands, note that the autocorrelation of the periodic part of $\tilde{m}^2(t)$ is given by $7/15 - 2/3 (r/T)^2$ $(1 - r/T)^2$ for $0 \leqslant r \leqslant T$. The normalized power in the desired lines is $4/9$, while the power in the sideband at $\pm k/T$ (Hz) is $1/(k\pi)^4$. Therefore, each of the first pair of sidebands is down about 16 db relative to the desired signal, and each of the second pair of sidebands is down 12-db further.

Recall that the frequency search range of the beacon receiver is ±1 kHz. The frequency doubling that occurs in the squarer results in an equivalent post-squarer search range of ±2 kHz. Since $1/T$ is 800 kHz, the first pair of sidebands, and at least one of the second pair of sidebands, will lie within the range of the frequency search. Because of the narrow post-squarer filter bandwidths, the receiver can detect the presence of, and phase-lock to, each of the first pair of sidebands at high P_r/N_o's. But the reference signal for the coherent detection of the beacon modulation is generated by frequency halving the phase-locked oscillator output, so this reference signal has an error of 400 Hz. The phasing of this signal is such that successively demodulated chips are inverted. Thus, if framing in slot S1 has one polarity, the sequence appearing in slot S2 will be inverted with respect to the polarity that it would have if the correct reference signal were used. The receiver timebase synchronization logic is arranged to detect this condition, and then to continue the search for the correct frequency.

APPENDIX C
FREQUENCY ACQUISITION

Section III. A. 1. a describes briefly the frequency search procedure whose chief advantage is adequate performance with little complexity. A detailed description of the basic scheme, and a comparison with other such methods, is given in Ref. C1. In this Appendix the basic analytic results are applied to the beacon receiver, the resulting parameter choices are described, and the analytic results are compared with the experimental results given in Section IV. A.

1. RESULTS OF REF. C1

The technique analyzed is an analog of the procedure followed to tune a superhet AM receiver. There, the listener varies the local oscillator frequency until he hears the desired station. In this search scheme the receiver local oscillator is varied linearly in frequency with time while the output of a narrowband energy detector is monitored. If the energy detector output exceeds a specified threshold, the sweep is turned off. If, after a fixed delay of T_1 seconds the receiver has not verified that a valid signal was detected (e.g., the receiver's phase-locked loop has failed to lock onto the incoming signal) the search is resumed. Such a strategy is necessary because the sweep may be turned off by spurious signals or noise bursts, in addition to the correct signal.

A block diagram of a bandpass realization of the acquisition scheme is given in Fig. C-1. The signal $\sqrt{2P_r} \cos \omega_c t$ is received in the presence of Gaussian noise whose real one-sided spectral density is N_o watts/Hz about ω_c. The voltage-controlled oscillator (VCO) output (while sweeping) is such that the difference frequency terms appearing at the output of the mixer are given by

$$d(t) = \sqrt{2P_r} \cos (1/2 \, Rt^2 + \omega_{IF} t + \Theta) + n_d(t) \quad .$$

$n_d(t)$, the translated version of the received noise, is modeled as white Gaussian noise of real density N_o watts/Hz.

Detection is defined as the event of the energy detector output $x^2(t)$ exceeding the threshold level L when the instantaneous angular frequency Rt is
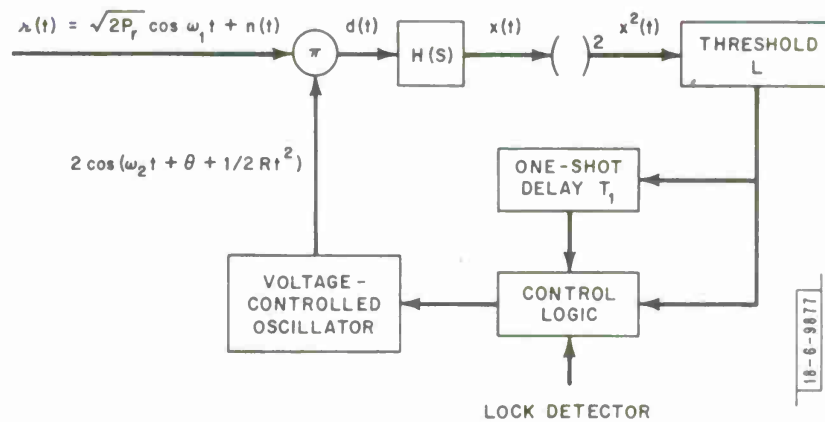
39

Fig. C-1. Bandpass model of acquisition system analyzed in Ref. C1. H(s) is a bandpass filter centered at ω_{IF}.

contained in the filter bandwidth W on any one sweep of the local oscillator. The equivalent lowpass transfer function of the filter $H(s)$ is $(W W_1)/(s + W) (s + W_1)$ with $W_1 \gg W$.

It was shown that best performance occurs when $W \simeq 1/2 \sqrt{R/2}$. Assuming such a filter bandwidth, an approximation to the probability of detection on a single sweep, P_D, is:

$$P_D \simeq Q(A/\sigma, \sqrt{L/\sigma}) \quad ,$$

where $Q(.,.)$ is Marcum's Q-function,

$$A^2/\sigma^2 = 2P_r/N_o \sqrt{R/2} \quad ,$$

$$\sigma^2 = (N_o W)/2 \quad .$$

The actual P_D is somewhat higher for high values of the approximation because the latter neglects the chance of detection occurring before or after maximum filter response.

During that portion of a sweep in which the signal is not contained within the $[W/(s + W)]$ $[W_1/(s + W_1)]$ passband, noise alone will occasionally drive the process $x^2(t)$ above the threshold L. Such events are of short duration, but the system waits an amount of time T_1 after $x^2(t)$ has dropped below L before continuing to sweep. This delay is included to facilitate the acquisition of fading signals and to provide sufficient time for verification of a detected signal. It was assumed that L is not exceeded again during the interval T_1 following the preceding dropout. The assumption is most accurate where the sweep is rarely turned off by noise alone, which is the case of primary interest.

Assuming that the probability density of the incoming frequency is uniform,

$$\overline{T}_{ACQ} \simeq \frac{[1/2 + (P_M/1 - P_M)] \, (W_A/R)}{\left\{ 1 - e^{-L/2\sigma^2} \left[1 + (W W_1 L/2\pi\sigma^2)^{1/2} \, T_1 \right] \right\}} \quad ,$$

41

where

$\overline{T}_{ACQ}$ = average acquisition time,

W_A = total range of uncertainty in rad/sec to be searched,

and

$P_M = 1 - P_D \simeq$ probability of failure to lock on a particular sweep.

Note: W_A/R is the duration of one uninterrupted sweep through W_A.

2. ADAPTATION TO BEACON RECEIVER

As described earlier, the beacon signal has very little carrier component. Therefore, the frequency acquisition subsystem must be preceded by the carrier reconstruction technique described in the text and Appendix B. To apply the foregoing results, P_r/N_o is replaced by P_s/N_s, the signal-to-noise-density out of the carrier reconstruction squarer. This substitution implies that the squarer output noise density is flat; in reality, the density falls off at frequencies greater than a matched filter bandwidth from the reconstructed carrier. Therefore, actual performance should be slightly better than the calculations indicate, but the improvement is not normally noticeable.

The carrier reconstruction squarer acts as a frequency doubler. Therefore, as far as the frequency acquisition system is concerned, the uncertainty search window W_A, and the sweep rate R, are effectively doubled. Thus, for example, in terms of the actual sweep rate,

$$A^2/\sigma^2 = 2P_s/N_s \sqrt{R} \quad .$$

The variation in P_D with P_s/N_s is rapid. Because P_s/N_s varies more rapidly than P_r/N_o in the region of interest, the change in P_D with P_r/N_o is very pronounced. In practical terms, the receiver experiences a sharp threshold effect.

It is desired to minimize the P_r/N_o consistent with the uncertainty window W_A, the average acquisition time $\overline{T}_{ACQ}$, and the pull-in delay T_1. Analytic

42

solutions for the minimum P_r/N_o, and the appropriate sweep rate R, were not obtained. However, $P_M = 0.1$ was chosen as threshold because it gives a reasonable tradeoff between the chance of missing the beacon signal on the first sweep, the required P_r/N_o, and the increase (22 percent) in $\overline{T}_{ACQ}$ over that when P_M is zero. Also, to reduce performance sensitivity to absolute gain and threshold settings, it is desirable that the percentage time the sweep is disabled by noise alone be small. This means the denominator of the expression for $\overline{T}_{ACQ}$ should be close to 1. After trying various values satisfying these conditions, the threshold design P_r/N_o of 29.5 db(Hz) was established for the beacon receiver, consistent with an average frequency acquisition time of 30 sec at P_r/N_o's greater than 30 db(Hz) Reduction of the threshold P_r/N_o by only 1 db would require that $\overline{T}_{ACQ}$ be doubled.

The frequency search threshold P_r/N_o is slightly greater than the minimum P_r/N_o required by the other beacon receiver subsystems. Thus if the "line" is detected at all, the receiver will complete acquisition successfully with very high probability.

To illustrate the rapid improvement in performance as P_r/N_o increases above threshold, Fig. C-2 presents the calculated probability of miss on a given sweep (P_M). Calculated and measured percentages of detection (P_D) on a single sweep are given in Fig. C-3. The experimental results do not conflict with the theory at and above threshold. Below the design threshold, the actual receiver degrades much more rapidly than indicated. This rapid degradation below threshold is believed due to the hardware approximations (half-linear multipliers approximating true multipliers, and linear rectifiers approximating square-law devices). These approximations are quite accurate at the design value of P_r/N_o, but are certainly not accurate over a large range of input levels.
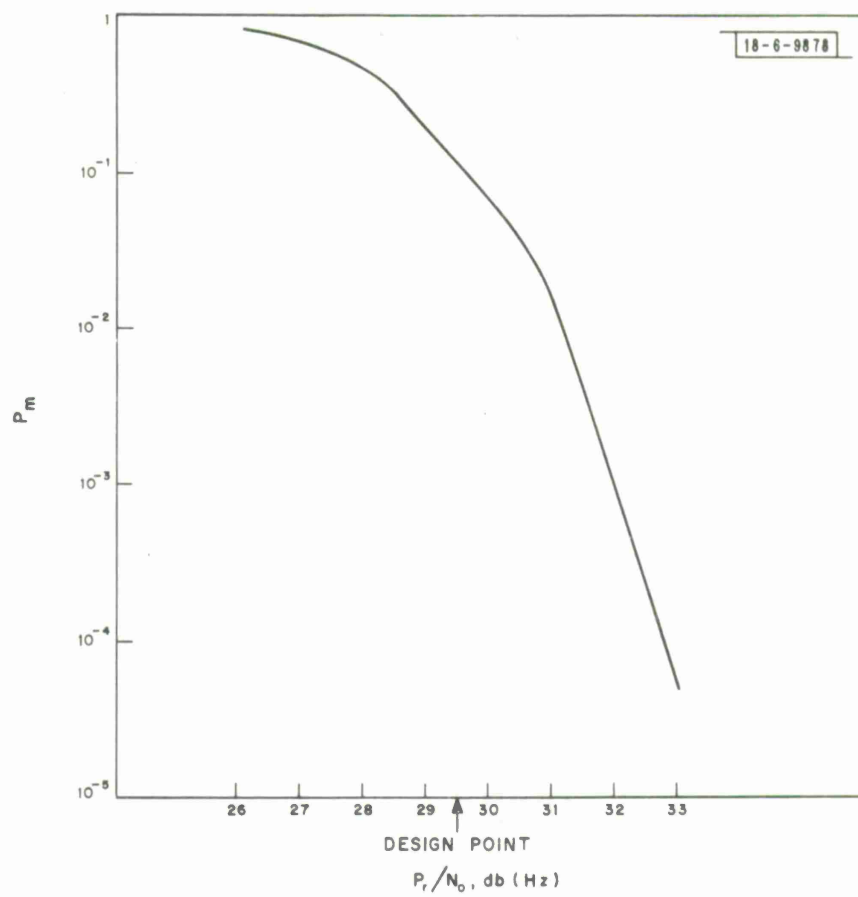
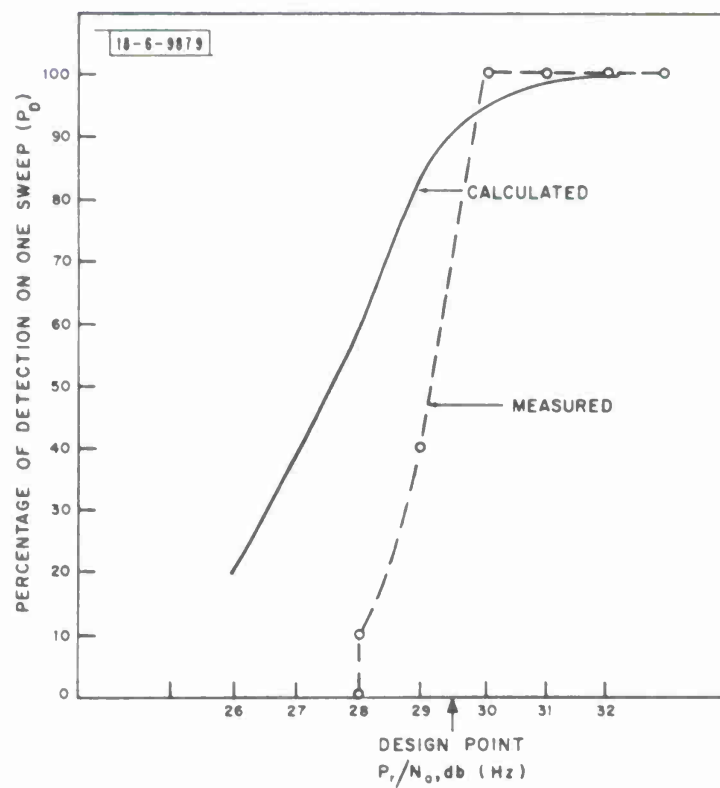Fig. C-2. Calculated beacon receiver performance.

Fig. C-3. Beacon frequency acquisition performance.

APPENDIX D
PHASE-LOCKING CONSIDERATIONS

The performance of the conventional beacon carrier-tracking phase-locked loop and the associated lock detector is described. Consideration is given to those issues that are not generally appreciated.

1. LOOP S/N REQUIREMENTS

The usual phase-locked loop configuration has a second-order loop filter $F(s) = 1 + A/s$. First-order loops were excluded from consideration because of poor tracking performance; loops of higher order than second are difficult to realize and may suffer from stability problems. A second-order loop with a damping ratio of $1/\sqrt{2}$, which is optimum for many criteria, is assumed. Then the loop-noise bandwidth W_L is related to the loop natural frequency ω_n by W_L(Hz) = $0.375 \sqrt{2} \omega_n$ (rad/sec). The effect of input noise is described by the linearized model phase variance $\sigma_\Theta^2 = (N_o/S)_L W_L$, where $(S/N_o)_L$ is the ratio of signal power to noise power in a 1-Hz band at the loop input. Assuming the received frequency is constant, cycle-slipping events become frequent for $\sigma_\Theta^2 > 0.25$, while they are negligible for $\sigma_\Theta^2 < 0.1$.

Transient behavior is described conveniently in terms of the steady state phase error occurring in an equivalent linearized loop for an input ramp of frequency. Let the rate of change of frequency be D_o Hz/sec. Then $\phi_{ss} = 2\pi D_o/\omega_n^2$ for a noise-free input.

Reasonable choices for a loop tracking in the presence of noise are $\phi_{ss} \leqslant 0.3$ and $\sigma_\Theta^2 \leqslant 0.1$. Such a loop may be expected to maintain lock down to $\sigma_\Theta^2 > 0.25$, if the input frequency is constant. Combining the above relations gives the required signal-to-noise ratio as

$$D_o \leqslant 0.0017 \, (S/N_o)_L^2 \quad .$$

Further discussion of basic loop performance is given in Refs. D1 and D2.

a. Squaring Loop (Acquire Mode)

The received signal is matched-filtered and squared; then the loop tracks the resulting double-frequency line. The signal-to-noise ratio $(S/N_o)_L = P_s/N_s$ out of the squarer and into loop was given in Fig. B-2 (Appendix B) as a function of E_c/N_o, where $E_c = P_r T$ is the energy per chip (1.25 msec) and N_o is the noise density at the squarer input. This model is reasonable as long as the loop noise bandwidth is much less than a matched filter bandwidth. Therefore, $W_L \leqslant 0.1/T$ is required. Because of the squaring, the appropriate doppler rate D_o for the tracking constraint is twice the doppler rate at the input. The resulting maximum doppler rate at the input to the receiver is plotted in Fig. D-1. This curve illustrates the very sharp variation in maximum tracking rate with P_r/N_o. The selected design point for 10 Hz/sec tracking gives a minimum P_r/N_o of about 29 db. The constant average envelope AGC preceding the carrier reconstruction circuit causes the effective signal amplitude (and thus the effective loop bandwidth) to vary with the received P_r/N_o so that the loop tracking performance approximates the optimum over a moderately wide range of P_r/N_o.[D3]

b. Coherent Loop (Monitor Mode)

The signal delivered to the loop is the received signal multiplied by the local replicas of the signals in slots S1 through S6. During slots S7 and S8 (spare and telemetry) the loop is disconnected. As long as the rate of disconnection is much greater than the loop bandwidth (say $W_L \leqslant 8/T$), the available $(S/N_o)_L$ is approximately P_r/N_o. However, since the input signal is available for only 3/4 of the time, the maximum input doppler rate is about 3/4 of the input doppler rate if the signal were continuous. The resulting maximum doppler rate is plotted in Fig. D-1. The curve illustrates the dramatic improvement in performance obtained by using the local replica of the beacon modulation.

2. PULL-IN

When the reconstructed carrier is detected within the energy detector filter bandwidth, the phase-lock loop circuitry is enabled and the loop pulls
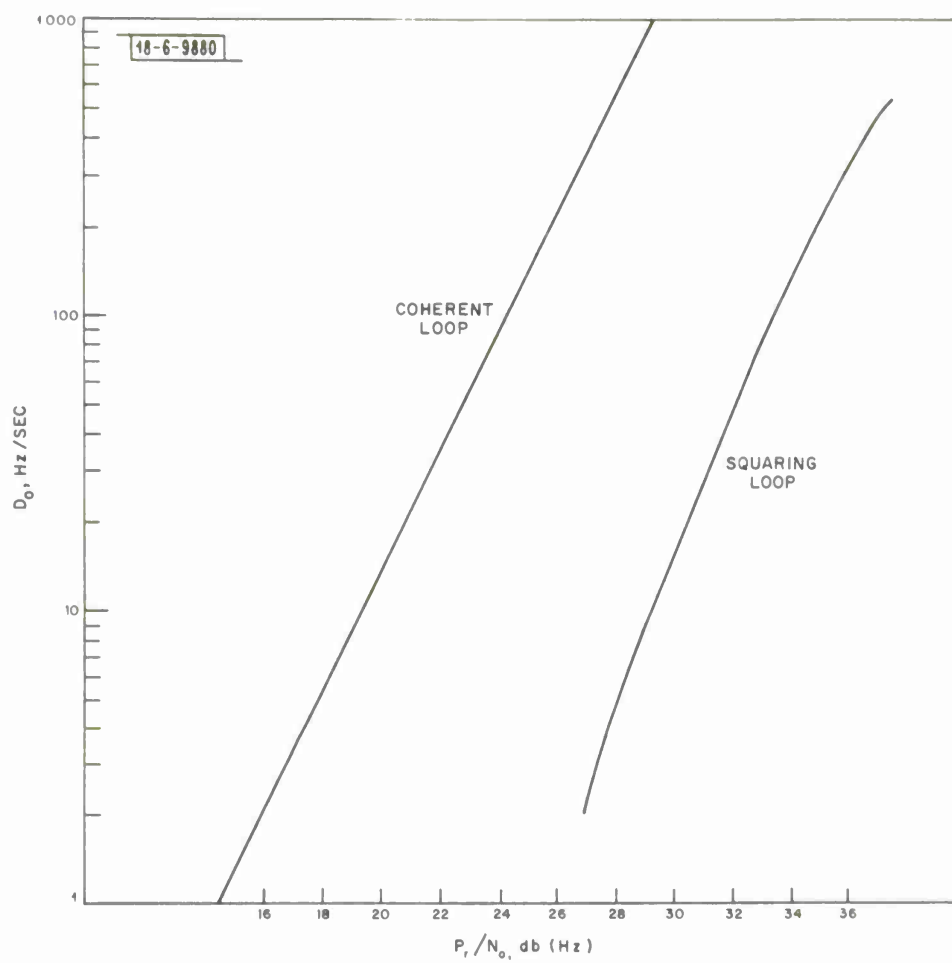
Fig. D-1.   Maximum tracking rates.

48

into phase lock. In a little known work[D4] it was shown that for an initial angular frequency error $5\omega_n$, a second-order loop with $\zeta = 0.7$ will lock within $33/\omega_n$ seconds, with a probability of greater than 0.95, for high loop signal to noise ratios ($\sigma_\Theta^2 \leqslant 0.1$). In terms of the actual loop parameters, this translates to lock within about 2 sec for an initial frequency error of 12 Hz, with a P_r/N_o of 29 db (Hz), with a probability of greater than 0.95. Since the 3-db bandwidth of the acquisition filter is about 3 Hz, the probability of phase acquisition after "line" detection is very high. At higher P_r/N_o's, the chance of a larger initial frequency error is greater because of the gradual falloff of the energy detector filter response, but this is offset by the greater effective loop bandwidth, so that overall performance is very reliable.

3.   OSCILLATOR STABILITY CONSIDERATIONS

A description of the effects of oscillator stability on phase-locked loop performance is given in Ref. D5. The major difficulty here is the lack of uniform meaningful standards of oscillator specification among the various manufacturers. It is hoped that the IEEE Committee on Definition of Frequency Stability will soon establish such standards.

Based on the known characteristics of well-engineered quartz crystal oscillators, an average fractional frequency deviation $\Delta f/f$ of 3×10^{-9} or less, for 10 msec averaging time, should give negligible loop performance degradation. Commercial VCXO's were purchased according to this specification and performed satisfactorily.

4.   LOCK DETECTION

Figure D-2 is a diagram of the lock detector under consideration. For analysis, the received signal is taken to be CW of power S watts observed in the presence of white additive Gaussian noise of real (one-sided) spectral density N_o watts/Hz. The equivalent signal into the lowpass filter is written as $s(t) + n(t)$, with $s(t) = \sqrt{2S} \cos \varphi$ while in phase lock with phase error φ, and $s(t) = 0$ for the case when the relative frequency error exceeds the passband of the lowpass filter. In normal operation the loop signal-to-noise ratio will be sufficiently high so that the approximation $\cos \varphi = 1$ is valid. This is assumed
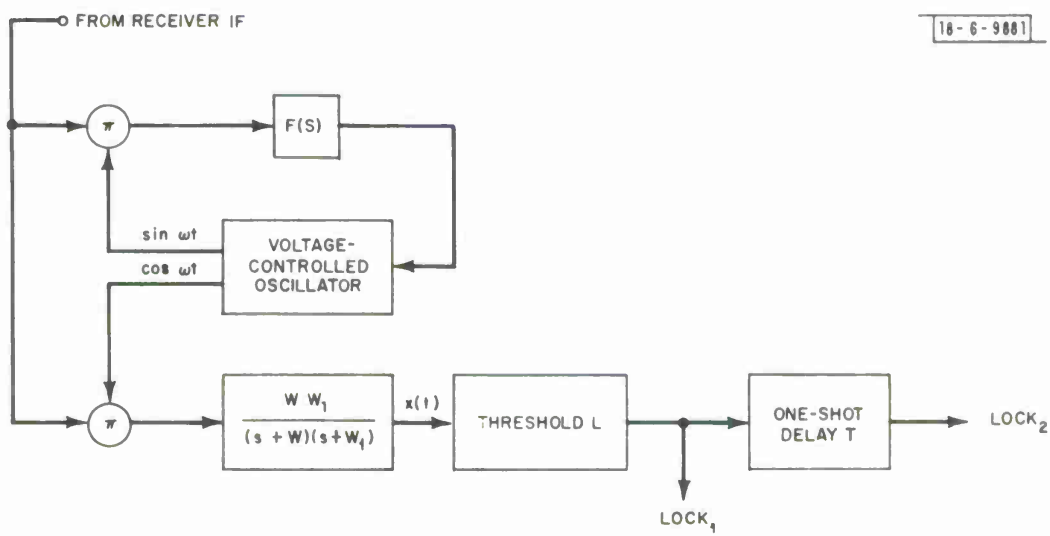
Fig. D-2.   Lock detector.

throughout the Note. The noise $n(t)$ has a flat two-sided spectrum of density N_o about $\omega = 0$; and the spectral density is zero for $|\omega| > 2\pi F$ radians, where F (which is very much greater than the lowpass filter bandwidth) is determined by, for example, the IF filter. The lowpass filter has a transfer function $WW_1/(s + W)(s + W_1)$.

The random process out of the filter $x(t)$ is modeled as Gaussian with zero mean when out of lock, and mean equal to $\sqrt{2S}$ when in lock. In both cases the variance $\sigma^2 \cong (N_o/2)(WW_1/W + W_1)$.

An output is present at "Lock$_1$" whenever $x(t) > L$. This signal is used as a direct indication of phase lock when the receiver is not searching in frequency. Lock$_2$ is always on when Lock$_1$ is on; in addition, it remains on for an interval of T seconds after Lock$_1$ goes off. Lock$_2$ is OR'ed with Lock$_1$. The resulting composite signal permits initiation of the search procedure if lock is lost due to severe frequency excursions of the received signal, but prevents short fades or occasional cycle-slipping from starting the search.

There are three events of primary interest:

a. During periods when phase lock is established, noise may occasionally drive $x(t)$ below L. It is desirable that this happen for only a small percentage of the time. A straightforward analysis gives the percentage time as $P_a = F[(\sqrt{2S}/\sigma) - (L/\sigma)]$, where

$$F(u) \equiv \frac{1}{\sqrt{2\pi}} \int_u^\infty e^{-x^2/2} \, dx \quad .$$

Tables of this function are widely available.

b. When the signal is lost, the receiver should initiate the search procedure after waiting T seconds. The probability that the search is initiated after only T seconds is the probability that noise alone does not exceed L during T seconds. To approximate this probability, note that about $N = WW_1 T/4\pi(W + W_1)$ independent samples of $x(t)$ could be taken in T seconds. Following an analysis similar to that of a., the probability that any one sample exceeds L is $P_b = F(L/\sigma)$. Then the probability that search is initiated after only T seconds is $(1 - P_b)^N$. To avoid excessive waiting times, it is desirable that this probability be on the order of, or greater than, $\frac{1}{2}$.

c. While locked, what is the probability (P_c) that the noise could force $x(t) < L$ for greater than T seconds? This would cause the receiver to initiate a frequency search incorrectly. Cramér and Leadbetter[D6] have shown that the probability density of the event $x(t) < L$ approaches $\pi/2 \, (t/\Theta) \, e^{-\pi/4 \, (t/\Theta)^2}$, where Θ is the average duration of the event. Integrating from T to ∞:

$$P_c \simeq \Theta \, e^{-\pi/4 \, (T/\Theta)^2}$$

where

$$\Theta = \sqrt{2\pi/WW_1} \, e^{u^2/2} \, F(u)$$

$$u = \sqrt{2S/\sigma} - L/\sigma \quad .$$

The approximation is increasingly accurate as u increases. It is clearly desirable that P_c be extremely low.

Performance in all three of the foregoing events improves as σ, or the equivalent bandwidth of the filter, decreases. On the other hand, it is desirable that the filter transient response be fast enough to permit the detection of most cycle-slipping events. Matching the filter time constant to the transient decay time of the linearized phase-locked loop gives $W = \zeta \omega_n = \omega_n/\sqrt{2}$. However, to ensure that the loop threshold dominated the lock detector threshold, the smaller value $W = \omega_n/2$ was selected. $W_1 = 10\,W$ was chosen for convenience. The ω_n used in these relations is the value applying at the loop design point $\sigma_\Theta^2 = 0.1$. L/σ was selected as 2. Then in the squaring mode the probability of starting a search correctly after loss of signal with no extra delay is greater than $\frac{1}{2}$, the probability of starting the search incorrectly is astronomically small (less than 10^{-10^4}), and the lock detector threshold falsely indicates the absence of a signal about 10^{-6} of the time at the design point, and about 0.03 of the time with a loop variance 4 db higher (the nominal loop threshold when the input frequency is constant). Similar results hold for the corresponding loop variance when in the coherent mode. The chosen parameters appear to be entirely satisfactory in practice.

APPENDIX E
TIME ACQUISITION

The LES-5 satellite radiates a biphase modulated beacon signal for communication terminal time synchronization. The beacon modulation is composed of 10-msec frames containing eight 1.25-msec chips. One chip in each frame, by definition the first chip, is always −1 to provide framing information. The second through sixth chips are samples from the outputs of pseudorandom sequence generators having relatively prime periods. The seventh chip is alternately 1 and −1, and the eighth chip contains telemetry information.

To obtain the timing information contained in the beacon modulation five local pseudorandom generators are synchronized to their satellite counterparts. This Appendix describes a particular sequential synchronization method. Assuming RF frequency and phase synchronization, the scheme operates as follows: First, a locally generated framing pulse is multiplied against the received modulation sequence. A fixed bias is subtracted from the product, and the resulting difference is integrated. The integrator output is continuously compared against two thresholds — the decision that framing alignment has been established corresponds to crossing the upper threshold, while the decision that the local framing pulse is not aligned to the received framing pulse corresponds to crossing the lower threshold. If the lower threshold is crossed, the local framing reference is shifted by half of a chip, the integrator is reset, and the test repeats. Once the local framing pulse has been aligned to the received framing pulse, the reference waveform becomes the output of the first pseudorandom sequence generator. The test structure is the same, but now the effect of crossing the lower threshold is to cause the local pseudorandom sequence generator to shift in time by one frame. This set of tests is repeated until all the local pseudorandom generators have been properly synchronized. Once framing has been established a fine time loop is enabled to reduce the difference between local time and the received waveform time to a very small fraction of one chip.
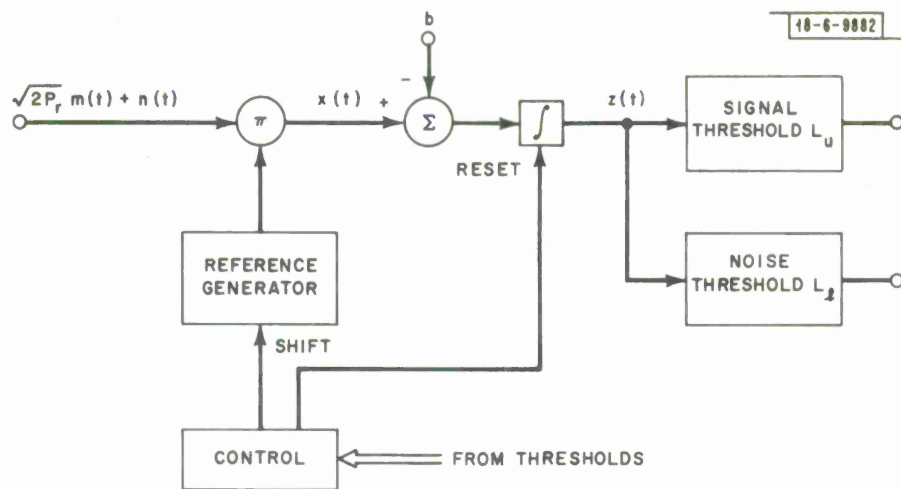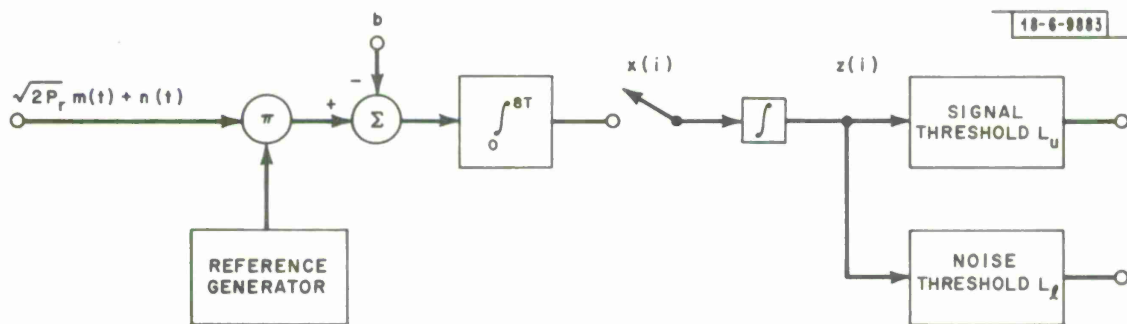
Fig. E-1.   Coarse time alignment system.

Fig. E-2.   Modified model of coarse time alignment system.

1.   Model

A block diagram of one step in the acquisition process is shown in Fig. E-1.
Figure E-2 gives a modified model that is more convenient for analysis, but
whose performance is essentially identical to that of the model in Fig. E-1.
The received signal is multiplied against the reference, a bias is subtracted,
and the result integrated for one frame interval.   (The multiplier output is zero
except during the chip interval under test.)   The output of the first integrator
is sampled and reset to zero at the end of each frame: the samples are inte-
grated in the second integrator whose output is compared with the signal (upper)
threshold L_u and noise (lower) threshold L_ℓ.   This quantization permits the re-
sults of Wald to be applied directly — the quantization is effectively eliminated
in the final results by permitting fractional sampling intervals in the calculation
of the average time to cross either threshold.

Let H_1 denote the event that the relative time alignment error is less than
one chip, and H_0 denote an event of greater relative time alignment error.   The
received signal is of the form $\sqrt{2P_r}\ m(t) + n(t)$ where $m(t)$, ± 1's, is the satel-
lite modulation sequence and $n(t)$ is white additive Gaussian noise of two-sided
spectral density N_o.

Now suppose the event H_1 holds with a fractional time misalignment
$\alpha = \tau_e/T$, where T is the duration of one chip and τ_e is the actual misalignment.
Then the samples $x(i)$ are given by $x(i)\,|\,H_1 = s - 8bT + n_1(i) + n_2(i)$ where s is
the DC component due to the cross-correlation between the reference and the
received waveform, $-8bT$ is the effect of the bias, $n_1(i)$ is the effect of the re-
ceived additive Gaussian noise, and $n_2(i)$ is the effect of intersymbol interfer-
ence due to imperfect alignment.   Clearly $s = (1 - \alpha)\sqrt{2P_r}\,T$, and the $n_1(i)$ may
be taken as independent zero-mean Gaussian random variables with variance
$N_o T$.   Assuming the adjacent pulse has positive or negative polarity with equal
probability, independent of the other components of $x(i)$, $n_2(i)$ is also uniquely
defined statistically.

In the sequel we shall be dealing only with sums of the $x(i)$, and the corre-
sponding sums of the $n_2(i)$ consequently have a binomial distribution.   This dis-
tribution is conveniently (and accurately) approximated by a Gaussian distribution.

But the distributions of the sums of the $n_2(i)$ would also be Gaussian if the in-dividual $n_2(i)$ were Gaussian. Therefore, for computational convenience, we may assume that the $n_2(i)$ are Gaussian with zero means and variances equal to $2P_r T^2 \alpha^2$. Equivalently, $n(i)|H_1 \overset{\triangle}{=} n_1(i) + n_2(i)$ is Gaussian with zero mean and variance $N_o T + 2P_r T^2 \alpha^2$.

On the other hand, if the time alignment error is greater than one chip, $x(i)$ consists of the bias plus noise:

$$x(i)|H_0 = -8bT + n(i)|H_0 = -8bT + n_1(i) + n_3(i)$$

The process $n_1(i)$ is modeled as above. $n_3(i)$ corresponds to $n_2(i)$, but has variance $2P_r T^2$. Therefore the $n(i)|H_0$ is taken as independent zero-mean Gaussian random variables with variances $N_o T + 2P_r T^2$.

In the following two sections the results of Wald are applied. Consult Ref. E1 for more details.

2.   Error Probabilities for a Single Test

Let $P_F = Pr[error|H_0]$ = probability of false alarm, and $P_M = Pr[error|H_1]$ = probability of miss. An error corresponds to the wrong threshold being crossed first. The occurrence of a false alarm results in the system believing that synchronization has been established when in fact it has not. On the other hand, occurrence of a miss means that the system had achieved synchronization, but didn't realize it. The first type of error is more serious for the beacon receiver in that it can lead to situations that drastically increase the average acquisition time. The second error is less serious in that the receiver will ordinarily repeat the search several times. Thus, if the system has probabil-ity of miss P_M on one search, the probability of missing N successive times is P_M^N.

Following Wald, let Θ_i be the solution of the Equation $\ln M(\Theta_i) = 0$, where $M(\Theta_i)$ is the moment generating function of the random variable $x(i)$ under the hypothesis H_1. For a Gaussian distribution with mean m and variance σ^2,

$$\Theta = -\frac{2m}{\sigma^2} \quad .$$

Therefore, using the means and variances from above

$$\Theta_0 = \frac{16bT}{N_o T + 2P_r T^2} \qquad\qquad > 0$$

$$\Theta_1 = \frac{16bT - 2(1-\alpha)\sqrt{2P_r}\,T}{N_o T + 2P_r T^2 \alpha^2} \qquad\qquad < 0 \quad .$$

Then

$$P_F = \frac{1 - e^{L_\ell \Theta_0}}{e^{L_u \Theta_0} - e^{L_\ell \Theta_0}}$$

$$P_M = \frac{1 - e^{L_u \Theta_1}}{e^{L_\ell \Theta_1} - e^{L_u \Theta_1}} \qquad . \qquad .$$

By manipulation one may show $P_F < e^{-L_u \Theta_0}$. The bound is approached for very small P_F. Since this is the region of interest, $P_F = e^{-L_u \Theta_0}$ is taken and it is remembered that the actual P_F should be slightly lower. If $|L_u \Theta_1| \gg 1$, $P_M \simeq e^{-L_\ell \Theta_1}$. This condition is satisfied for the parameters used in the beacon receiver.

Taking logs of both equations and substituting,

$$\ln \frac{1}{P_F} = \frac{16b}{N_o + 2P_r T} L_u$$

and

$$\ln \frac{1}{P_M} = \frac{16b - 2(1-\alpha)\sqrt{2P_r}}{N_o + 2P_r T \alpha^2} L_\ell$$

3.   Average Acquisition Time and Probability of Acquisition

Let n be the number of samples taken from the output of the first integrator before either threshold is crossed. We allow n to be a continuous random

variable to avoid (artificial) difficulties due to quantization of n. Let Z be the value of output of the integrator. Then $E(n) = E(Z)/E[x(i)]$. Applying this fundamental result of Wald

$$E[n \,|\, H_0] = \frac{P_F L_u + (1 - P_F) L_\ell}{-8bT}$$

$$E[n \,|\, H_1] = \frac{P_M L_\ell + (1 - P_M) L_u}{(1 - \alpha) \sqrt{2P_r} T - 8bT} \quad .$$

Operating with $P_F \ll 1$, the first expression may be reduced to

$$E[n \,|\, H_0] \simeq \frac{L_\ell}{-8bT} \quad .$$

Solving the expressions for P_F and P_M to get L_u and L_ℓ, and substituting,

$$E[n \,|\, H_0] = \frac{N_o + 2P_r T\alpha^2}{16bT[(1 - \alpha)\sqrt{2P_r} - 8b]} \; \ln\left(\frac{1}{P_M}\right)$$

$$E[n \,|\, H_1] \simeq \frac{N_o + 2P_r T\alpha^2}{2T[(1 - \alpha)\sqrt{2P_r} - 8b]^2} \; P_M \, \ln\left(\frac{1}{P_M}\right)$$

$$+ \frac{N_o + 2P_r T}{16bT[(1 - \alpha)\sqrt{2P_r} - 8b]} \; (1 - P_M) \, \ln\left(\frac{1}{P_F}\right) \quad .$$

Now, let $\overline{T} \,|\, H_i$ denote the average time to test one alignment. Then

$$\overline{T} \,|\, H_i = E[n \,|\, H_i] \times [\text{sampling period of } 1^{\text{st}} \textstyle\int = 8T] \quad .$$

Substituting,

$$\overline{T} \,|\, H_0 = \text{average time spent testing a wrong delay for a single sequence}$$

$$= \frac{N_o + 2P_r T\alpha^2}{2b[(1-\alpha)\sqrt{2P_r} - 8b]} \ln\left(\frac{1}{P_M}\right) \quad ;$$

$\overline{T}|H_1 =$ average time spent testing the correct delay for a single sequence

$$= \frac{N_o + 2P_r T\alpha^2}{[(1-\alpha)\sqrt{2P_r} - 8b]^2} 4P_M \ln\left(\frac{1}{P_M}\right)$$

$$+ \frac{N_o + 2P_r T}{2b[(1-\alpha)\sqrt{2P_r} - 8b]} (1 - P_M) \ln\left(\frac{1}{P_F}\right) \quad .$$

To calculate overall acquisition performance, it is first necessary to consider the effect of a fractional time error α different from the design value. Let $\wedge$ denote the design value of a variable. From the expression $P_M \simeq e^{-I_\ell \Theta_1}$ this is (for constant $\widehat{E_c/N_o}$)

$$P_M \simeq (\hat{P}_M)^{\Theta_1/\hat{\Theta}_1}$$

where

$$\Theta_1/\hat{\Theta}_1 = \left[2\frac{1-\alpha}{1-\hat{\alpha}} - 1\right]\left[\frac{1 + 2\hat{\alpha}^2 E_c/N_o}{1 + 2\alpha^2 E_c/N_o}\right] \quad .$$

The beacon receiver design point (acquisition mode) is $\hat{\alpha} = \frac{1}{2}$ and $E_c/N_o = 0$ db, giving

$$\Theta_1/\hat{\Theta}_1 = [3 - 4\alpha]\left[\frac{3/2}{1 + 2\alpha^2}\right] \quad .$$

Now recall that framing is shifted in $\frac{1}{2}$-chip increments, so that if correct alignment is not detected at a particular (correct) value of α, it can also be detected with α increased by $\frac{1}{2}$ (also correct). Combining this fact with the above variation of P_M with α, it is concluded that the probability of failing to

59

acquire framing during one test of all positions is less than $(\hat{P}_M)^5$ at the design value of E_c/N_0. Similarly, the probability of failing to acquire the sequence in either slot S2 or slot S3 during one test of all positions is less than $(\hat{P}_M)^2$ for each slot. For the other slots, the fine time loop will have reduced the fractional error substantially, so that the probability of failing to acquire the sequence in each of slots S4, S5, and S6 is less than $(\hat{P}_M)^3$ each. Furthermore, the receiver logic is arranged so that the receiver tests each position at least twice (assuming failure during the first test). It follows that the probability of successful acquisition is somewhat greater than

$$P_{ACQ} \simeq (1 - \hat{P}_M^{10})\,(1 - \hat{P}_M^{4})^2\,(1 - \hat{P}_M^{6})^3$$

$$\simeq 1 - 2\hat{P}_M^{4} \quad .$$

This probability is much closer to 1 if the initial fractional time error is much less than $\frac{1}{2}$.

Because of the complex behavior of P_M as a function of α, it is not practical to calculate the exact average acquisition time. However, for any one sequence j let there be N_j possible delay positions, and let the probability of the correct delay being in any one position be $1/N_j$. Let $\overline{T}_{SEQ_j}$ be the average time to synchronize sequence j. Then, by assuming that there are at most two possible delay positions which are correct, that the probability of miss in each position is $\hat{P}_M$, and that the average duration of the test in each of the correct positions is $\overline{T}|H_1$, an upper bound on the true value is

$$\overline{T}_{SEQ_j} < \frac{1 + \hat{P}_M^{2}}{1 - \hat{P}_M^{2}}\,\frac{N_j - 2}{2}\,\overline{T}|H_0 + \frac{1}{1 - \hat{P}_M^{2}}\,\frac{1 + 2\hat{P}_M}{1 + \hat{P}_M}\,\overline{T}|H_1 \quad .$$

A lower bound is given by the assumption of perfect detection:

$$\overline{T}_{SEQ_j} > \frac{N_j - 2}{2}\,\overline{T}|H_0 + \overline{T}|H_1 \quad .$$

The bounds differ by about 20 percent at $\hat{P}_M = \frac{1}{4}$, and the upper approaches the

lower as $\hat{P}_M$ decreases. The upper bound is used below to obtain a conservative design.

Let $\overline{T}_{SYNC}$ be the average time to establish synchronization for the total of J sequences so

$$\overline{T}_{SYNC} = \sum_{j=1}^{J} \overline{T}_{SEQ_j} \quad .$$

Substituting for $\overline{T}|H_0$ and $\overline{T}|H_1$, a direct but tedious computation shows that $\overline{T}_{SYNC}$ is minimized by $8\hat{b} = \frac{1}{2}(1 - \hat{\alpha})\sqrt{2P_r}$ when $K \gg J$, which is the case of interest, where

$$K \triangleq \frac{1}{2} \sum_{j=1}^{J} N_j \quad .$$

This minimum is:

$$\overline{T}_{SYNC} \simeq \frac{8T}{(1 - \alpha)^2} \left[\frac{N_o}{E_c} + 2\alpha^2 \right] \left[\frac{1 + P_M}{1 - P_M} (K - J) \right.$$

$$+ \frac{P_M(1 + 2P_M)}{(1 - P_M)(1 + P_M)^2} J \left] \ln\left(\frac{1}{P_M}\right) + \frac{8T}{(1 - \alpha)^2} \right.$$

$$\times \left[\frac{N_o}{E_c} + 2 \right] \frac{1 + 2P_M}{(1 + P_M)^2} J \ln \frac{1}{P_F} \quad .$$

For LES-5, $N_1 = 32$, $N_2 = 25$, $N_3 = 27$, $N_4 = 29$, $N_5 = 31$, $N_6 = 32$, $J = 6$, and $K = 88$. N_1 comes from the fact that framing is tested in $\frac{1}{2}$-chip increments, and both polarities must be tested. N_2 through N_6 are the periods of the respective pseudorandom sequence generators. Detection is desired at $\frac{1}{2}$-chip error, so $\hat{\alpha} = \frac{1}{2}$. Substituting, with $8T = 10$ msec and $E_c/N_o = 0$ db,

61

$$\overline{T}_{SYNC} \simeq 0.12 \left[41 \frac{1 + P_M}{1 - P_M} + 3 \frac{P_M + 2P_M^2}{1 + P_M - P_M^2 - P_M^3} \right] \ln \frac{1}{P_M}$$

$$+ 0.72 \frac{1 + 2P_M}{(1 + P_M)^2} \ln \frac{1}{P_F} \quad .$$

The design point was chosen as $P_M = 0.36$ and $P_F = 10^{-5}$, giving $\overline{T}_{SYNC} \simeq 18$ sec, and the probability of failing to successfully acquire with $\alpha = 1/2$ less than 0.03. Since the initial value of α is approximately uniform, the true probability of failing to successfully acquire timing is very much less.

4. Other Signal-to-Noise-Density Ratios

The autocorrelation functions of the beacon timing sequences have substantial minor peaks. In the worst case, if the main peak is 1, the largest minor peak (magnitude) is $-7/32$. Now at high P_r/N_o's, the frequency search can detect and phase lock with a constant 400 Hz error, so that successive sequences (as seen by the time demodulator) are inverted. Thus with a fixed bias, the time section could incorrectly indicate that the inverted sequences were properly aligned. To avoid this problem, the bias current fed into the time acquisition integrator is derived from the lock detector circuit, rising above the design value as the P_r/N_o increases. This variable bias also causes P_F and P_M to decrease as P_r/N_o increases, giving overall performance better than that which would result from a fixed bias.

5. Monitor Mode

Once synchronization has been established, the receiver switches over to monitor mode. The alignment of each sequence is continually checked just as in acquisition mode. However, if the noise threshold L_ℓ is crossed, the test is repeated up to 64 times. The resulting probability of missing a sequence is then P_M^{64}, where P_M is the probability of miss on a single test. If the noise threshold is crossed 64 consecutive times, the time section reverts to the acquisition mode described above.

62

The operation of the fine time loop is such that α should be approximately zero while the receiver is operating in the monitor mode. Thus P_M is substantially decreased. The result is that P_M^{64} is less than 10^{-10} at a P_r/N_o of 20 db (Hz).

ACKNOWLEDGMENTS

REFERENCES

1. B. E. Nichols and W. W. Ward, "Lincoln Experimental Satellite-5 (LES-5) Transponder Performance in Orbit," Technical Note 1968-18, Lincoln Laboratory, M.I.T. (1 November 1968).

2. B. E. Nichols, private communication.

3. G. Ploussios, "Noise Temperature of Airborne Antennas at UHF," Technical Note 1966-59, Lincoln Laboratory, M.I.T. (6 December 1966), DDC 644829.

4. C. A. Lindberg, "A Shallow-Cavity UHF Crossed-Slot Antenna," Technical Report 446, Lincoln Laboratory, M.I.T. (8 March 1968), DDC 672763.

5. K. L. Jordan, "Measurement of Multipath Effects in a Satellite-Aircraft UHF Link," IEEE Proc. 55, 6, 117-118 (June 1967).

6. A. Johnson, "Six Month Report of Flight Test Results," Program 591, Aeronautical Systems Division and Air Force Avionics Laboratory, Wright-Patterson AFB, Ohio (July – December 1967).

7. L. I. Bluestein, "Interleaving of Pseudorandom Sequences for Synchronization," IEEE Trans. AES-4, 4, 551-556 (July 1968).

A1. J. W. Craig, "RLC Realizations of Approximations to Matched Filters for a Rectangular Pulse," Technical Note 1968-21, Lincoln Laboratory, M.I.T. (30 July 1968), DDC 673883.

A2. J. P. Costas, "Synchronous Communications," IRE Proc. 1713 (31 August 1956).

B1. J. W. Layland, "An Optimum Squaring Loop Prefilter," JPL Space Programs Summary 37-37, IV (28 February 1966).

C1. T. Seay, "Swept Frequency Acquisition," (to be published).

D1. A. J. Viterbi, Principles of Coherent Communication (McGraw-Hill, New York, 1966).

D2. F. M. Gardner, Phaselock Techniques (Wiley, New York, 1966).

D3. R. Jaffe and E. Rechtin, "Design and Performance of Phase-Lock Circuits Capable of Near-Optimum Performance over a Wide Range of Input Signal and Noise Levels," IRE Trans. Information Theory IT-1, 66-76 (March 1955).

D4. R. J. McLaughlin, "A Lock-on Probability Analysis for the Initial Synchronization of Phase-Locked Loops," Technical Report 372, Cruft Laboratory, Harvard University (3 February 1963).

D5. T. Seay, "Short Term Oscillator Stability Specifications for Phase-Locked Loops," Technical Note 1968-5, Lincoln Laboratory, M.I.T. (29 April 1968), DDC 669090.

D6. H. Cramer and M. R. Leadbetter, Stationary and Related Stochastic Processes (Wiley, New York, 1967).

E1. A. Wald, Sequential Analysis (Wiley, New York, 1947).

Security Classification

DOCUMENT CONTROL DATA – R&D

(Security classification of title, body of abstract and indexing annotation must be entered when the overall report is classified)

1. ORIGINATING ACTIVITY *(Corporate author)*	2a. REPORT SECURITY CLASSIFICATION
Lincoln Laboratory, M.I.T.	Unclassified
	2b. GROUP
	None

3. REPORT TITLE

A LES-5 Beacon Receiver

4. DESCRIPTIVE NOTES *(Type of report and inclusive dates)*

Technical Note

5. AUTHOR(S) *(Last name, first name, initial)*

Seay, Thomas S. and Huntoon, Albert H.

6. REPORT DATE	7a. TOTAL NO. OF PAGES	7b. NO. OF REFS
1 May 1969	72	17

8a. CONTRACT OR GRANT NO. AF 19(628)-5167	9a. ORIGINATOR'S REPORT NUMBER(S)
b. PROJECT NO. 649L	Technical Note 1969-27
c.	9b. OTHER REPORT NO(S) *(Any other numbers that may be assigned this report)*
d.	ESD-TR-69-76

10. AVAILABILITY/LIMITATION NOTICES

This document has been approved for public release and sale; its distribution is unlimited.

11. SUPPLEMENTARY NOTES	12. SPONSORING MILITARY ACTIVITY
None	Air Force Systems Command, USAF

13. ABSTRACT

A functional description of a communications satellite beacon receiver is presented. The system, designed primarily for LES-5/6, is capable of reliable unattended operation, and provides a frequency and time reference for fixed and highly mobile satellite communications terminals.

Theoretical and experimental data are given, with particular emphasis on automatic acquisition and tracking of the satellite beacon signal at low signal-to-noise-density ratios under adverse channel conditions.

14. KEY WORDS

UHF beacon receiver mobile satellite communications terminal	LES-5 LES-6